

Journal Pre-proof

Discovery of a promising agent IQZ23 for the treatment of obesity and related metabolic disorders

Yong Rao, Zhao Xu, Yu-Tao Hu, Chan Li, Yao-Hao Xu, Qin-Qin Song, Hong Yu, Bing-Bing Song, Shuo-Bin Chen, Qing-Jiang Li, Shi-Liang Huang, Jia-Heng Tan, Tian-Miao Ou, Hong-Gen Wang, Guo-Ping Zhong, Ji-Ming Ye, Zhi-Shu Huang

PII: S0223-5234(20)30139-2

DOI: <https://doi.org/10.1016/j.ejmech.2020.112172>

Reference: EJMECH 112172

To appear in: *European Journal of Medicinal Chemistry*

Received Date: 4 December 2019

Revised Date: 18 February 2020

Accepted Date: 19 February 2020

Please cite this article as: Y. Rao, Z. Xu, Y.-T. Hu, C. Li, Y.-H. Xu, Q.-Q. Song, H. Yu, B.-B. Song, S.-B. Chen, Q.-J. Li, S.-L. Huang, J.-H. Tan, T.-M. Ou, H.-G. Wang, G.-P. Zhong, J.-M. Ye, Z.-S. Huang, Discovery of a promising agent IQZ23 for the treatment of obesity and related metabolic disorders, *European Journal of Medicinal Chemistry* (2020), doi: <https://doi.org/10.1016/j.ejmech.2020.112172>.

This is a PDF file of an article that has undergone enhancements after acceptance, such as the addition of a cover page and metadata, and formatting for readability, but it is not yet the definitive version of record. This version will undergo additional copyediting, typesetting and review before it is published in its final form, but we are providing this version to give early visibility of the article. Please note that, during the production process, errors may be discovered which could affect the content, and all legal disclaimers that apply to the journal pertain.

© 2020 Published by Elsevier Masson SAS.



Title page

Discovery of a Promising Agent IQZ23 for the Treatment of Obesity and Related Metabolic Disorders

Yong Rao^{a, †, *}, Zhao Xu^{a, †}, Yu-Tao Hu^a, Chan Li^a, Yao-Hao Xu^a, Qin-Qin Song^a, Hong Yu^a, Bing-Bing Song^a, Shuo-Bin Chen^a, Qing-Jiang Li^a, Shi-Liang Huang^a, Jia-Heng Tan^a, Tian-Miao Ou^a, Hong-Gen Wang^a, Guo-Ping Zhong^c, Ji-Ming Ye^b, Zhi-Shu Huang^{a, *}

^a Guangdong Provincial Key Laboratory of New Drug Design and Evaluation, School of Pharmaceutical Sciences, Sun Yat-Sen University, Guangzhou, Guangzhou 510006, China

^b Molecular Pharmacology for Diabetes Group, School of Health and Biomedical Sciences, RMIT University, Melbourne, VIC, 3083 Australia

^c Laboratory of Drug Metabolism and Pharmacokinetics, School of Pharmaceutical Sciences, Sun Yat-Sen University, Guangzhou, China.

*To whom correspondence should be addressed. Tel.: 8620-39943056, Fax: 8620-39943056, E-mail addresses: raoyong0805@126.com (Y. Rao), ceshzs@mail.sysu.edu.cn (Z.-S. Huang).

† These authors contributed equally

Abstract

Discovery of novel anti-obesity agents is a challenging and promising research area. Based on our previous works, we synthesized 40 novel β -indoloquinazoline analogues by altering the skeleton and introducing preferential side chains, evaluated their lipid-lowering activity and summarized the structure-activity relationships. In combination with an evaluation of the lipid-lowering efficacies, AMP-dependent activated protein kinase (AMPK) activating ability and liver microsomal stability, compound **23** (named as **IQZ23**) was selected for further studies. **IQZ23** exerted a high efficacy in decreasing the triglyceride level ($EC_{50} = 0.033 \mu\text{M}$) in 3T3-L1 adipocytes. Mechanistic studies revealed the lipid-lowering activity of **IQZ23** was dependent on the AMPK pathway by modulating ATP synthase activity. This activation was accompanied by mitochondrial biogenesis and oxidation capacity increased, and insulin sensitivity enhanced in pertinent cell models by various interventions. Correspondingly, **IQZ23** (20 mg/kg, *i.p.*) treatment significantly reversed high fat and cholesterol diet (HFC)- induced body weight increases and accompanying clinical symptoms of obesity in mice but without indicative toxicity. These results indicate that **IQZ23** could be a useful candidate for the treatment of obesity and related metabolic disorders.

KEYWORDS

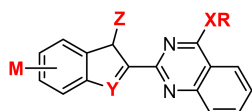
synthesis; 3T3-L1 adipocyte; AMPK activation; obesity; metabolic disorders.

Abbreviations

ACC: acetyl-CoA carboxylase; ACSL: long-chain acyl-CoA synthetase; AMP: adenosine 5'-monophosphate; AMPK: adenosine 5'-monophosphate activated protein kinase; ATP: adenosine-triphosphate; C/EBP α : CCAAT-enhancer binding proteins α ; CH: chow diet; CPT-1 β : carnitine palmitoyl transterase-1 β ; FAS: fatty acid synthase; GTT: glucose tolerance test; H&E: hematoxylin-eosin staining; HFC: high fat and cholesterol diet; ITT:

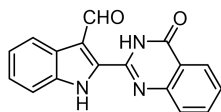
insulin tolerance test; LDH: lactate dehydrogenase; 2-NBDG: 2-deoxy-2-[(7-nitro-2,1,3-benzoxadiazol-4-yl)amino]-D-glucose; NRF2: nuclear factor erythroid-2-related factor 2; OCR: oxygen consumption ratio; ORO: oil-red O; PGC-1 α : peroxisome proliferator activated receptor gamma coactivator-1 α ; PI3K: phosphatidylinositol 3'-kinase; PPAR γ : peroxisome proliferator-activated receptor γ ; SCD-1: stearyl-CoA desaturase 1; SREBP-1c: sterol responding element binding protein-1c; TFAM: transcription factor A mitochondria; TG: triglyceride.

Journal Pre-proof



40 novel derivatives (1-40)

↑
Structural modification

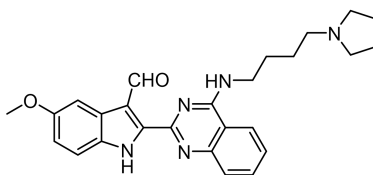


Bouchardatine

EC_{50} in 3T3-L1 = 25 μ M

→
Screening and evaluating

- Lipid-lowering activity
- AMPK activating ability
- Liver microsomal stability



IQZ23

In 3T3-L1 adipocyte:

EC_{50} = 0.036 μ M, IC_{50} > 50 μ M;

In microsomal:

$t_{1/2}$ = 187 min;

Aqueous solubility = 73.3 μ g/mL;

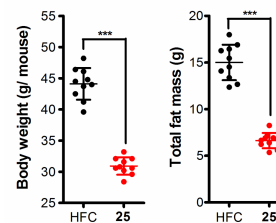
PK assay:

F = 48.6%; C_{max} = 37.1 ng/mL; T_{max} = 4 h.



HFC

IQZ23



Journal Pre-proof

Title page

Discovery of a Promising Agent IQZ23 for the Treatment of Obesity and Related Metabolic Disorders

Yong Rao^{a, †, *}, Zhao Xu^{a, †}, Yu-Tao Hu^a, Chan Li^a, Yao-Hao Xu^a, Qin-Qin Song^a, Hong Yu^a, Bing-Bing Song, Shuo-Bin Chen^a, Qing-Jiang Li^a, Shi-Liang Huang^a, Jia-Heng Tan^a, Tian-Miao Ou^a, Hong-Gen Wang^a, Guo-Ping Zhong^c, Ji-Ming Ye^b, Zhi-Shu Huang^{a, *}

^a Guangdong Provincial Key Laboratory of New Drug Design and Evaluation, School of Pharmaceutical Sciences, Sun Yat-Sen University, Guangzhou, Guangzhou 510006, China

^b Molecular Pharmacology for Diabetes Group, School of Health and Biomedical Sciences, RMIT University, Melbourne, VIC, 3083 Australia

^c Laboratory of Drug Metabolism and Pharmacokinetics, School of Pharmaceutical Sciences, Sun Yat-Sen University, Guangzhou, China.

*To whom correspondence should be addressed. Tel.: 8620-39943056, Fax: 8620-39943056, E-mail addresses: raoyong0805@126.com (Y. Rao), ceshzs@mail.sysu.edu.cn (Z.-S. Huang).

Abstract

Discovery of novel anti-obesity agents is a challenging and promising research area. Based on our previous works, we synthesized 40 novel β -indoloquinazoline analogues by altering the skeleton and introducing preferential side chains, evaluated their lipid-lowering activity and summarized the structure-activity relationships. In combination with an evaluation of the lipid-lowering efficacies, AMP-dependent activated protein kinase (AMPK) activating ability and liver microsomal stability, compound **23** (named as **IQZ23**) was selected for further studies. **IQZ23** exerted a high efficacy in decreasing the triglyceride level ($EC_{50} = 0.033 \mu\text{M}$) in 3T3-L1 adipocytes. Mechanistic studies revealed the lipid-lowering activity of **IQZ23** was dependent on the AMPK pathway by modulating ATP synthase activity. This activation was accompanied by mitochondrial biogenesis and oxidation capacity increased, and insulin sensitivity enhanced in pertinent cell models by various interventions. Correspondingly, **IQZ23** (20 mg/kg, *i.p.*) treatment significantly reversed high fat and cholesterol diet (HFC)- induced body weight increases and accompanying clinical symptoms of obesity in mice but without indicative toxicity. These results indicate that **IQZ23** could be a useful candidate for the treatment of obesity and related metabolic disorders.

KEYWORDS

synthesis; 3T3-L1 adipocyte; AMPK activation; obesity; metabolic disorders.

Abbreviations

ACC: acetyl-CoA carboxylase; ACSL: long-chain acyl-CoA synthetase; AMP: adenosine 5'-monophosphate; AMPK: adenosine 5'-monophosphate activated protein kinase; ATP: adenosine-triphosphate; C/EBP α : CCAAT-enhancer binding proteins α ; CH: chow diet; CPT-1 β : carnitine palmitoyl transterase-1 β ; FAS: fatty acid synthase; GTT: glucose tolerance test; H&E: hematoxylin-eosin staining; HFC: high fat and cholesterol diet; ITT:

insulin tolerance test; LDH: lactate dehydrogenase; 2-NBDG: 2-deoxy-2-[(7-nitro-2,1,3-benzoxadiazol-4-yl)amino]-D-glucose; NRF2: nuclear factor erythroid-2-related factor 2; OCR: oxygen consumption ratio; ORO: oil-red O; PGC-1 α : peroxisome proliferator activated receptor gamma coactivator-1 α ; PI3K: phosphatidylinositol 3'-kinase; PPAR γ : peroxisome proliferator-activated receptor γ ; SCD-1: stearoyl-CoA desaturase 1; SREBP-1c: sterol responding element binding protein-1c; TFAM: transcription factor A mitochondria; TG: triglyceride.

Journal Pre-proof

1. Introduction

Diet and lifestyle contribute to the high incidence of obesity in developed and developing countries. Currently, approximately 65% of the adult population is overweight, with a body mass index of greater than or equal to 25 kg/m^2 , and over 30% of the adult population is obese (body mass index of greater than or equal to 30 kg/m^2) [1]. Over the past 3 decades, the number of overweight and obese individuals global is increasing exponentially, especially in Europe, America and other countries and the number have increased over 1 billion [2]. Obesity is associated with an increased risk for diabetes mellitus, cancer, and heart disease, and it often causes a shortening of human life and economic burdens [3]. Advances in the treatment of obesity have thus far been rather limited with few drugs available to control abnormal fat accumulation [4]. Most anti-obesity agents are based on altering the appetite by acting on receptors in the brain. Some drugs in this class (such as fenfluramine) have been withdrawn from the market due to their unexpected toxicity or physical side effects [5]. Recent attempts to develop compounds that inhibit the absorption of fat through the gastrointestinal tract (such as orlistat) may improve anti-obesity treatment. Nevertheless, even the most effective drugs can only reduce body weight by up to 5%, and strict dieting is required for further weight loss [4]. Apart from these treatments, promoting energy expenditure is another approach to the treatment of obesity and associated diseases [6].

AMP-dependent activated protein kinase (AMPK) is a master metabolic regulator and maintains energy homeostasis by regulating the balance between catabolism and anabolism involved in all branches of cellular metabolism. AMPK's activation is dependent on energy status and upstream kinase, such as liver kinase B1 (LKB1) and CaMKK (Calcium/calmodulin-dependent protein kinase kinase). In relation to metabolic diseases, the activation of AMPK has been shown to play a vital role

in increasing glucose uptake, fatty acid oxidation (FAO), mitochondrial biogenesis, and autophagy, while suppressing the synthesis of fatty acids, cholesterol, and protein [7, 8]. Regarding these beneficial effects, several direct or indirect AMPK activators have shown efficacy in ameliorating obesity and related clinical syndromes [9, 10], and recently some of them have been included in clinical trials, such as Metabolaid and ActivAMP [11, 12].

Indole and quinazoline are common drug pharmacophores, and their derivatives have extensive bioactivities, such as anticancer, resistant to chronic obstructive pulmonary disease, and anti-hepatitis. They have been characterized as “dominant structures” in drug design since they have strong affinities with some receptors. Several compounds containing indole and quinazoline were reported to have efficacy in treating obesity and diabetes, such as **I3C** and **KZL-1** [13, 14]. Our preliminary studies have indicated that the natural alkaloid bouchardatine (Figure 1) ameliorated high-fat diet (HF) induced obesity in mice (~14.6% decrease in body weight) *via* regulating energy metabolism [15]. In addition, a series of derivatives were synthesized and some of them, such as compound **R17** (Figure 1), were reported to significantly improve its lipid-lowering activity [16, 17], as well as anti-obesity activity in mice (data not shown), further indicating that these β -indoloquinazoline analogues should be considered as promising molecules for treating obesity and related metabolic disorders. Thus, it would be of great significance to develop more detailed information on the structure-activity relationships (SARs) of these analogues and on candidates likely to respond well to drug therapy for obesity and related metabolic disorders.

In this study, to explore new molecules with high lipid-lowering activity and good druglike properties, 4 series of novel β -indoloquinazoline analogues (totally 40 compounds) were designed and synthesized based on the structures of our previous β -indoloquinazoline derivatives (Figure 1).

First, to analyze the importance of NH (at 13-position) in the indole ring, we replaced the NH with an oxygen atom, or introduced a substitute (methyl or benzyl group) at the nitrogen atom, to give 7 compounds for Series I (1–7). Second, we further expanded the types of side chain at the 5-position by changing the NH into an oxygen or sulfur atom, to generate 10 compounds for Series II (8–17). Third, we introduced a methoxy group at 10-position to improve water-solubility and bioavailability and to give 6 compounds for Series III (18–23). Finally, we replaced the aldehyde group at the 8-position with a methyl group to further check the necessity of the aldehyde group, since our previous studies have confirmed that the replacement of the aldehyde with a halogen group would affect the activity of the compounds [18]; meanwhile, we also replaced the NH at the 13-position with an oxygen or sulfur atom, to produce 17 compounds for Series IV (24–40). Their biological activities and SARs were investigated. After combinational screening assays including the efficacies in triglyceride (TG) decreasing and AMPK activating, as well as liver microsomal stability, the best compound was further evaluated. We assessed lipid-lowering activity, adipocyte differentiation, and lipid synthesis inhibitory activities *via* AMPK activation, improvement of insulin sensitivity and mitochondrial biogenesis, pharmacokinetics properties, and anti-obesity and associated metabolic disorders effects using a mouse model induced by a high fat and cholesterol diet (HFC).

2. Results and discussion

2.1 Chemistry.

To improve the lipid-lowering activity, physicochemical properties, and further explore the SARs, we designed and synthesized four series of compounds (totally 40 new compounds) based on our preliminary studies [17, 18]. The synthetic routes and chemical structures of the target compounds

are shown in Scheme 1 and Table 1, respectively. Ethyl 3-methylbenzofuran-2-carboxylate (**a**), originated from the reaction with 2-hydroxyacetophenone and ethyl bromoacetate and was treated with sodium hydroxide solution to obtain the carboxylic acid **b**. The intermediate **b** was prepared into the carbonyl chloride to react with 2-aminobenzamide to give **c**, which was subjected to intramolecular cyclization to get the intermediate **d**. Compound **d** was reacted with NBS to give the bromides **e** which then reacted with DMSO to produce the intermediate **f**. The compound **g**, by chlorinating the carbonyl group of **f**, reacted with the desired amine to get the Series I compounds (**1–5**). The intermediate **h** was prepared by 2-aminobenzamide according to the preliminary literature procedure [15], and it was introduced into the methyl or benzyl group at the nitrogen atom of the indole ring to get the intermediates **i** and **j**, respectively, followed by substitution and formylation to get Series I compound **6** and **7**. 1*H*-indole-2-carboxylic acid (**k** and **l**) was reacted with oxalyl chloride to give the corresponding acyl chloride and then reacted with 2-aminobenzamide in one-pot to generate the intermediates **m** and **n**, respectively. The compound **m** could be formylated and chlorinated in one-pot by the treatment of POCl₃ and DMF to give the compound **o**. We added the amines, thiols or alcohols with different alkaline terminal groups to obtain the series II compounds (**8–17**). Similarly, starting from compound **n**, through the intermediate **p**, the series III compounds (**18–23**) could be obtained. The key intermediate **r** was prepared according to the literature procedure [16]. In addition, the intermediate **s** was prepared by a similar reaction with the preparation of **m** from starting material **q**. The series IV compounds (**24–40**) were synthesized by compounds **d**, **r**, and **s** treated with POCl₃ and DMF (to give compounds **t**, **u**, and **v**, respectively), followed by the amines or alcohols *via* nucleophilic substitution.

2.2 Evaluation of the Lipid-Lowering Activity of the Derivatives Using the 3T3-L1 Adipocyte Model.

By using the 3T3-L1 adipocyte cell model, the lipid-lowering activities of all the newly synthesized compounds were evaluated, and the SAR was concluded.

As shown in Figure 2A and Table S1, after a 6-day stimulation using the adipogenic cocktail (a mixture of dexamethasone, insulin, and IBMX), triglyceride (TG) levels in mature adipocytes were highly elevated, with a 5-fold increase compared to undifferentiated (UND) cells. As reported, treatment by compound **R17** significantly reversed the stimulation of the adipogenic cocktail as indicated by an approximate decrease of 79.2% and 89.3% in TG levels at 1 and 5 μM [16, 17], respectively, compared with differentiation (Control, Ctrl) cells. Meanwhile, metformin, a well-known AMPK activator, as positive control also led to a decrease of 60.3% in TG level at a concentration of 1 mM. It was shown that most of the newly synthesized compounds were effective in inhibiting lipid synthesis and accumulation in a dose-dependent manner. Among them, 11 of the 40 compounds showed a reduction of over 50% in TG levels at a concentration of 1 μM . Especially, 4 compounds (**11**, **20**, **21**, **23**) showed an equal or an improved lipid-lowering efficacy compared with **R17** at the concentration of 1 μM . Furthermore, The TG inhibitory effects of compound **11**, **20**, **21**, and **23** were also confirmed by Oil-red O (ORO) staining (Figure 2B). To exclude the adverse effect of cytotoxicity, we determined the cytotoxicity of these derivatives at the concentration of 5 μM in 3T3-L1 adipocytes after 6 days of incubation by lactate dehydrogenase (LDH) releasing assay. As noted, the incubation of all the derivatives did not alter the LDH releasing levels in the culture medium when compared with Ctrl cells (Figure S1), demonstrating that these derivatives were well-tolerated by 3T3-L1 adipocytes at the concentration of 5 μM , and the lipid-lowering activity of these derivatives was not due to their toxicity.

Based on the evaluation results, the SAR was summarized as follows. First, we found that the NH

group in the indole ring could be important. As shown in Figure 2A and Table S1, an obvious reduction of TG level suppression was observed in Series I compounds. For example, with replacement of the NH at 13-position of compound **10** with an oxygen atom to give compound **5**, the TG level went from 34.9% to 88.7% at 1 μ M, and with substitution of hydrogen for the NH of the positive compound **R17** with methyl for compound **6** and benzyl group for compound **7**, the TG levels went from 20.8% to 70.4% and 57.1%, respectively. Second, we investigated the effect of the NH group at the 5-position. It was shown that the replacement of NH (such as **R17**, **10**, and **3a** [17]) at the 5-position with oxygen (**14**, **17**, and **13**, respectively) or sulfur atom (**8**) would be unfavorable for the lipid-lowering activity of the compounds. Moreover, it was found that the length of the side chain also affected the activity. Third, the introduction of a methoxy group at the 10-position (Series III compounds **18–23**) seems to be beneficial for the decrease of the TG level since the TG contents were kept at a lower level (10.1 ~48.8%) after treatment with the five compounds compared with those of compounds without a methoxy group. Finally, we explored the importance of the aldehyde group. For Series IV compounds (**24–40**), replacement of the aldehyde group at the 8-position with a methyl group and/or the NH group at 13-position with an oxygen or sulfur atom, it was shown that the lipid-lowering activity of derivatives was decreased when the aldehyde group changed into a methyl group.

2.3 Evaluation of Adipocytes Differentiation Inhibition and AMPK Activation of 6 Potent Compounds.

On the basis of lipid-lowering activity and the SAR of the compounds above, we selected 4 potent molecules (**11**, **20**, **21**, and **23**) for additional studies. In the first experiments, the 4 compounds, plus **R17** for comparison, were tested for their needed concentration for 50% of maximal effect (EC_{50}) on

decreasing TG levels. As shown in Figure 3A, the treatment of derivatives at 0, 0.01, 0.1, 0.3, 1, 3, and 10 μM concentrations yielded dose-dependent decreases in TG levels in 3T3-L1 adipocytes, with EC_{50} values being at 0.51 μM , 0.92 μM , 0.31 μM and 0.033 μM , respectively. Specifically, compound **23** has a higher efficacy in decreasing TG levels compared with **R17** as judged by a comparable EC_{50} value (0.033 μM vs 0.091 μM).

Studies have revealed that adipocyte maturation is regulated by a network of genes that strictly initiate the processes of adipogenesis and lipogenesis [18]. Among them, adipogenic factors, such as CCAAT/enhancer-binding protein β , δ , and α (C/EBP β , δ , and α) and peroxisome proliferator-activated receptor γ (PPAR γ), play an essential role in controlling the early stage of adipocyte differentiation, namely, adipogenesis, which is followed by an activation of lipogenesis. Coinciding with the TG-decreasing effect, we next determined the effects of these potent derivatives on the expression level of adipogenic factors. Firstly, 1 mM of metformin treatment efficiently decreased the expression level of C/EBP (β , δ , α) and PPAR γ (Figure S2A). Cell treated with our derivatives dose-dependently blocked the stimulation of the adipogenic cocktail as indicated by decreases in the mRNA level of C/EBP (δ , β , α) and PPAR γ after 24 h incubation (Figure 3B-3E). In comparison with **R17**, compound **23** showed a stronger inhibition effect at each concentration in blocking the activation of these adipogenic markers, which were well related to the TG decreasing ability. Notably, at a lower concentration of 0.01 μM , **23** treatment exerted a higher efficacy in blocking the activation of these adipogenic markers.

Our previous studies have demonstrated that the β -indoloquinazoline derivatives which could inhibit adipocyte differentiation in cells and ameliorate obesity-related metabolic disorders in mice were association with an activation of the AMPK pathway [8]. We next determined the stimulation

effect of these derivatives on AMPK. **R17** and metformin (**Met**) were loaded as a positive control. As expected, both **R17** and **Met** treatment significantly increased the phosphorylated level (Thr-172) of AMPK α , and activated AMPK pathway (Figure S2B). Cells treated with the 4 derivatives also significantly increased the activity of AMPK in 3T3-L1 adipocytes as indicated by an increment in the phosphorylated level of AMPK α , and **23** showed a more enhanced effect on AMPK activity than **R17**. And compound **23** supplemented yielded a higher efficacy in activating AMPK pathway at each concentration compared with **R17**-treated cells (Figure 3F and Figure S2B). In light of the data, there seems to be a positive correlation between AMPK activation and TG-lowering activity, compounds with higher activity on AMPK activation yielding a higher efficacy in decreasing TG levels (Figure S2C).

2.4 Assay of Aqueous Solubility and Liver Microsomal Stability of 6 Potent Compounds.

To understand the druggability of the compounds, we further determined the aqueous solubility and liver microsomal stability of the 4 most potent compounds. As shown in Table 2, compared with **R17**, compounds **20**, **21**, and **23**, which introduced a methoxy group at 10-position, showed an increase in aqueous solubility, demonstrating that the introduction of methoxy is prone to improve the aqueous solubility of derivatives. Especially compared with **R17**, the water-solubility of compound **23** with the best lipid-lowering activity was significantly improved from 41.1 to 73.3 $\mu\text{g/mL}$. For the liver microsomal stability assay, testosterone was selected as a control compound. As shown in Table 2, compound **11**, **20**, **23** showed better stability in Sprague Dawley (SD) rat liver microsomal in comparison with **R17**. We next determined the stability of the most potent derivative **23** in different species microsomal, including dog, monkey and human liver microsomal. These results indicated that **23** was stable enough as indicated by the values of $t_{1/2}$ were 187.3, 630.1,

1155.2 and 630.1 min, respectively (Table 2, Figure S3). Furthermore, pharmacokinetics assay revealed that **23** had similar orally bioavailability and more favorable maximum plasma drug concentration compared with **R17** (Table 3), and also had less individual difference among mice. This improved pharmacokinetics feature of **23** may partly due to its increase in aqueous solubility [19, 20]. In conclusion, we selected compound **23** (named as **IQZ23**) as a hit compound from the library for further study.

2.5 **IQZ23** Blocked Adipocytes Differentiation Related to AMPK Pathway Activation.

As reported, 3T3-L1 pre-adipocytes differentiate into mature white adipocytes by undergoing three pivotal stages, namely, adipogenesis (Day 0-3), lipogenesis (Day 3-6) and terminal differentiation (Day 6-9). During the stage of adipogenesis, the adipogenic factors, such as C/EBP α , PPAR γ , and SREBP-1c, are activated in a time-dependent manner, which is followed by an initiation of lipogenesis by increasing the expression of fatty acid synthesis related proteins [21]. Studies have demonstrated that the interruption of adipogenesis was an effective approach to block the maturation of 3T3-L1 adipocytes [22]. Correspondingly, cells treated with **IQZ23** decreased TG levels in adipocytes in a time-dependent manner as indicated by an approximate decrease of 74.2%, 61.8% and 35.3% during the periods of Day 0-3, 3-6 and 6-9, respectively. Furthermore, there was no major difference in the TG level while **IQZ23** was incubated during the periods of Day 0-3, 0-6 and 0-9 (Figure 4A, Figure S4A), demonstrating that **IQZ23** inhibited adipocyte differentiation by interrupting the stage of adipogenesis. Western blot assays revealed that **IQZ23** treatment markedly decreased the protein level of adipogenic factors C/EBP α , PPAR γ , and sterol regulatory element-binding protein 1c (SREBP-1c) after 24 h treatment as well as the level of fatty acid synthesis related proteins fatty acid synthase (FAS), acetyl CoA carboxylase (ACC), stearoyl-CoA

desaturase 1 (SCD1) after 6 days of treatment (Figure 4B-C). The inhibition of adipogenic markers was also observed in metformin-treated cells (Figure S2A). It is worth noting that **IQZ23** showed a stronger inhibitory effect on these proteins compared with **R17** at a concentration of 1 μ M, which accorded with the TG-decreasing effect in 3T3-L1 adipocytes.

Moreover, cells treated with **IQZ23** and **R17** moderately blunted ATP synthase activity, decreased ATP levels and thus increased the ratio of AMP-to-ATP (Figure 4D-F). These changes in ATP levels and AMP-to-ATP ratio accorded well with AMPK activation (Figure 3F). To reveal the relationship between AMPK activation and the TG-decreasing effect mediated by **IQZ23**, 3T3-L1 adipocytes were transfected with AMPK α siRNA (50 nM) in the presence or absence of **IQZ23**. Knockdown of AMPK α blocked AMPK activation and efficiently abolished the stimulation effect of **IQZ23** on the AMPK pathway. This abolishment of AMPK activation led to a reversal in the protein level of C/EBP α , PPAR γ and TG level in 3T3-L1 adipocytes when compared with **IQZ23** treatment alone (Figure 4G-H, Figure S4B), suggesting that **IQZ23** blocked 3T3-L1 adipocyte differentiation *via* AMPK activation.

2.6 **IQZ23** Improved Insulin Sensitivity in C2C12 Myoblasts via the AMPK Pathway.

Studies have linked AMPK activation with the stimulation of glucose uptake and utilization in muscles and the liver, which are pivotal for maintaining glucose and insulin homeostasis and often malfunction due to obesity [8, 23]. As shown in Figure 5A-B, similar to insulin, both **R17** and **IQZ23** and also metformin alone treatment significantly increased glucose uptake (red foci) in C2C12 cells by 2-NBDG assay, an additive effect in glucose uptake was observed in the combination of drug and insulin compared with drug or insulin alone, and **IQZ23** showed a slightly enhanced effect in improving insulin sensitivity compared with **R17** in the presence or absence of insulin.

Moreover, the stimulation effect of **R17** and **IQZ23** was in parallel with AMPK pathway activation while no major change was observed in the total and phosphorylated (Ser-308) levels of AKT (Protein kinase B) (Figure 5C), which plays a key role in insulin-mediated phosphatidylinositol 3'-kinase (PI3K)/AKT pathway activation. Moreover, PI3K pathway inhibitor LY-294002 addition was able to block glucose uptake and the phosphorylated (Ser308) level of AKT in C2C12 cells, while its addition did not abolish the stimulation of **IQZ23** on glucose uptake as well as the activation of AMPK (Figure 5D-E). These results strongly demonstrated that **IQZ23** stimulated glucose uptake in C2C12 myoblasts through the AMPK pathway rather than the insulin-signaling pathway.

2.7 **IQZ23** Increased Mitochondria Oxidation Capacity.

Another important beneficial effect mediated by AMPK activation is mitochondria biogenesis and oxidative capacity increase, which burns and consumes fatty acids [24]. AICAR, a classic AMPK activator, was viewed as a control compound. As expected, AICAR, **R17** and **IQZ23** treatment increased mitochondria copy number (red foci) in 3T3-L1 adipocytes. This stimulation effect of AICAR, **R17**, and **IQZ23** were partially blocked by addition of AMPK pathway inhibitor Compound C (CC) (Figure 6A-B). Moreover, cells treated with **R17** and **IQZ23** activated the expression of mitochondria biogenesis markers (PGC-1 α , TFAM) and a network of genes indicative of mitochondrial oxidation capacities, such as CPT-1 β , ACSL, and NRF2 (Figure 6C). Correspondingly, mitochondrial oxidation capacity in **R17** and **IQZ23** treated cells was increased as indicated by an increment in oxygen consumption in 3T3-L1 adipocytes using an extracellular Flux Analyzer (Figure 6D).

2.8 **IQZ23** Ameliorated HFC Induced Obesity and Related Metabolic Disorders.

To assess whether **IQZ23** exerts *in vivo* therapeutic effects on obesity and related metabolic syndromes devoid of the influence on calorie intake, we used a high fat (60%) containing 1% cholesterol diet (HFC) induced mouse model to evaluate the anti-obesity, anti-hypoglycemic and anti-hypolipidemic effects of **IQZ23**. After 8 weeks of induction, mice were randomly divided into two subgroups, and one group of mice received vehicle treatment (HFC saline group), while another group of mice was treated with 20 mg/kg of **IQZ23** (HFC-**IQZ23** group) by intraperitoneal (*i.p.*) injection every other day for 6 weeks.

As shown in Figure 7A-B and Figure S5A, HFC-feeding induced a large increase in body weight compared to the group fed with chow diet (CH group) and **IQZ23** administration significantly reversed the increase in body weight to the level of the chow group mice as indicated by a 27.4% decrease compared with vehicle-treated mice. The body weight reduction was accompanied by a large decrease in fat mass content and lean mass in **IQZ23** treated mice (Figure 7C, Figure S5B). Consistent with the reduction of fat mass, **IQZ23**-treated mice displayed a marked reduction in the size of adipocytes as indicated by hematoxylin-eosin (H&E) staining of white adipose tissue (Figure S5C). Interestingly, the total food intake over 6 weeks in the **IQZ23**-treated group showed no major difference compared with the vehicle-treated mice (Figure 7D), indicating that the anti-obesity effect of **IQZ23** is not mediated by limiting calorie intake.

Next, we measured relevant plasma parameters and tissue weights to examine whether there was any indication of toxicity. Of note, HFC-feeding induced an increase in the size of organs and no major difference was observed in **IQZ23**-treated mice regarding the weight of the tissues studied when compared with vehicle-treated mice, while a significant decrease was observed in the weight of

livers in **IQZ23**-treated mice (Figure S5D). **IQZ23** administration also significantly reversed the increase in the activity of serum alanine aminotransferase (ALT) and aspartate transaminase (AST) as well as total bilirubin (TBIL), albumin (ALB), blood urea nitrogen (BUN) and creatine (CRE) after 14 weeks of HFC stimulation (Table 4). Moreover, acute toxicity experiments revealed the half lethal dose (LD₅₀) of **IQZ23** in mice is over 500 mg/kg in mice, indicating that **IQZ23** was well-tolerated *in vivo*.

Dyslipidemia and hyperglycemia are the main clinic syndromes that often accompany obesity [8]. As expected, mice treated with **IQZ23** had large decreases in plasma levels of free fatty acids (FFA), TG, glucose, insulin, LDL-c as well as the ratio of LDL-c/HDL-c, to a similar level to that of chow mice (Table 4). At the same time, we also determined the acute effect of **IQZ23** on improved hyperglycemia. HFC feeding mice were injected with **IQZ23** once, plasma glucose was decreased in a time-dependent manner, and an obvious anti-hyperglycemic effect occurred 6 h post-injection (Figure 7E). Consistent with this, GTT and ITT experiments further confirmed the anti-obesity effect of **IQZ23** in mice. After **IQZ23** administration, the mean area under curve (AUC) of GTT and ITT in **IQZ23**-treated mice was much lower than that of the vehicle-treated mice (Figure 7F-G), strongly indicating the effectiveness of **IQZ23** for treating of obesity and relevant metabolic disorders.

Nonalcoholic fatty liver disease (NAFLD) is a common metabolic disorder accompanying obesity, and it is characterized by lipid ectopic accumulation (FFA flux and glucose-induced lipogenesis) leading to hepatocyte injury in the liver [25]. Notably, mice treated with **IQZ23** experienced reduced liver weight and TG levels (Figure 8A-B). H&E and ORO staining assays further confirmed the efficacy of **IQZ23** in protecting the liver from hepatic steatosis (Figure 8C). These results were in agreement with a reduction in AST and ALT activities (Table 4).

3. Conclusions

In the present study, we synthesized 4 novel β -indoloquinazoline analogues (a total of 40 compounds) by altering skeleton structures or introducing preferential side chains and substitutes based on our previous findings.^{15, 17} The lipid-lowering activity of these compounds was tested, and the SAR was summarized in line. Based on the evaluation of the efficacies in lipid reduction, liver microsomal stability, aqueous solubility, and AMPK activation, **IQZ23** was selected as the most potent candidate for further study of the molecular mechanism and evaluation of the anti-obesity effect. Of note, an introduction of methoxy at the 10-position was effective at improving aqueous solubility, stability and pharmacokinetic properties of indoloquinazoline analogues, such as **IQZ23**. In cells, **IQZ23** was effective at decreasing lipid content with an EC₅₀ value of 0.036 μ M. This TG-decreasing effect was associated with AMPK activation by blunting ATP synthase activity and decreasing ATP levels. Furthermore, compared to controls, **IQZ23** treatment improved insulin sensitivity in myoblasts and increased mitochondrial oxidation capacity in adipocytes, all of which were beneficial effects accompanying AMPK activation for treating obesity. Accordingly, administration of **IQZ23** significantly reversed HFC induced body weight and fat mass increases. Analyses of plasma and liver revealed that **IQZ23** treatment significantly ameliorated obesity-induced dyslipidemia, hyperglycemia, and hepatic steatosis without indications of toxicity *in vivo*. Pharmacokinetics studies and liver microsomal assays demonstrated that **IQZ23** was more stable and soluble with a preferable bioavailability (~48.6%) *in vitro*, which was better than control compound **R17**. As shown above, **IQZ23** should be taken into consideration as a potential anti-obesity agent for treating obesity and related metabolic disorders.

4. Experimental section

4.1. Chemistry

All commercial chemicals used as starting materials were analytical grade and utilized without further purification. ^1H and ^{13}C NMR spectra were recorded using TMS as the internal standard in $\text{DMSO-}d_6$, $\text{MeOD-}d_4$ or CDCl_3 with a Bruker Avance III spectrometer at 400 MHz; Mass spectra (MS) were recorded on Agilent 6120 Quadrupole LC/MS instrument with an ESI mass selective detector, and high-resolution mass spectra (HRMS) were recorded on Shimadzu LCMS-IT-TOF. All synthesized compounds were purified by using flash column chromatography with silica gel (200-300 mesh). The purities of synthesized compounds were confirmed to be higher than 95% by using analytical HPLC equipped with a dual pump Shimadzu LC-20AB system with an AnalaRic C18 column (4.6×250 mm, $5 \mu\text{m}$), which was eluted with methanol-water (50:50 to 85:15, v:v) at a flow rate of $0.5 \text{ mL}\cdot\text{min}^{-1}$. Melting points (m.p.) were determined by using capillary tubes with an MSRS-OptiMelt automated melting point instrument without correction.

Ethyl 3-methylbenzofuran-2-carboxylate (a). To a stirred suspension of 2-hydroxyacetophenon (5.4 g, 40 mmol) in DMF(16 mL) was added ethyl bromoacetate (20 g, 120mmol) and potassium carbonate(22.1 g, 160 mmol), and the mixture was stirred at $80 \text{ }^\circ\text{C}$ for 1 h, and then up to $160 \text{ }^\circ\text{C}$ for 2 h. After the reaction solution was cooled, it was poured into a large amount of water and extracted with dichloromethane three times. The organic phase was washed with saturated sodium chloride solution for three times, dried with anhydrous sodium sulfate and removed the solvent under vacuum to give the crude product, which was then purified by using column chromatography with dichloromethane/petroleum ether, resulting in oil compound (3.2 g, 38.4%). ^1H NMR (400 MHz, CDCl_3) δ 7.62 (d, $J = 6.6$ Hz, 1H), 7.54 (d, $J = 8.3$ Hz, 1H), 7.44 (t, $J = 7.7$ Hz, 1H), 7.29 (t, $J = 7.9$

Hz, 1H), 4.50 – 4.41 (q, $J = 7.5$ Hz, 2H), 2.59 (s, 3H), 1.43 (t, $J = 7.1$ Hz, 3H). MS (ESI + APCI) m/z : 205.1 $[M+H]^+$.

3-Methylbenzofuran-2-carboxylic acid (b). The compound **a** was added to the mixture of a mixture of 2 M NaOH (20 mL) and methanol (30 mL), stirring at room temperature for 4 h. Removing methanol under vacuum, regulating the pH to 1 with concentrated hydrochloric acid, precipitating a large number of white solid, and extracting three times by ethyl ether, and finally removing the organic phase. It resulted in solid (1.77g, 99%). ^1H NMR (400 MHz, CDCl_3) δ 10.85 (s, 1H), 7.69 (d, $J = 7.8$ Hz, 1H), 7.60 (d, $J = 8.4$ Hz, 1H), 7.51 (t, $J = 7.7$ Hz, 1H), 7.35 (t, $J = 7.5$ Hz, 1H), 2.67 (s, 3H). MS (ESI + APCI) m/z : 177.1 $[M+H]^+$.

N-(2-Carbamoylphenyl)-3-methylbenzofuran-2-carboxamide (c). The intermediate **b** (0.7 g, 3.98 mmol) dissolving in sulfoxide chloride (6 mL), was stirred at 82 °C for 2 h. After the reaction solution cooling, removing sulfoxide chloride under vacuum to give the light green solid. It was dissolved in dichloromethane, following to drop into the solution of aminophenolamide (0.54 g, 4 mmol) in dichloromethane (20 mL) at ice-bath for 10h. The dichloromethane was removed by filtration. The crude was washed with a small amount of ethanol, and dried to obtain a white solid (0.89 g, 83%). MS (ESI + APCI) m/z : 295.1 $[M+H]^+$.

2-(3-Methylbenzofuran-2-yl)quinazolin-4(3H)-one (d). The compound **c** (0.89 g, 3.03 mmol) was added to the mixture of 2 M KOH and ethanol (v =1:1) at 80°C for overnight. Removing ethanol under vacuum, regulating the pH to 3 with diluted hydrochloric acid and filtering to give a large number of white solid (0.7 g, 80%). ^1H NMR (400 MHz, $\text{DMSO-}d_6$) δ 8.10 (d, $J = 7.7$ Hz, 1H), 7.73 (d, $J = 7.6$ Hz, 2H), 7.69 (d, $J = 7.2$ Hz, 1H), 7.65 – 7.58 (m, 2H), 7.46 – 7.41 (m, 1H), 7.39 (t, $J = 7.5$ Hz, 1H), 7.34 (t, $J = 7.4$ Hz, 1H), 2.75 (s, 3H). MS (ESI + APCI) m/z : 277.1 $[M+H]^+$.

2-(3-(Dibromomethyl) benzofuran-2-yl) quinazolin-4(3H)-one (e). The compound **d** (1 g, 3.62 mmol) dissolving in CCl₄ (60 mL) was added NBS (1.61 g, 9.05 mmol) and catalytic amount of benzoperoxide. Then it was heated at 90 °C for 24 h. The CCl₄ was removed by using a rotary evaporator. The residue was purified by using column chromatography with dichloromethane/petroleum ether to give compound **e** (0.8 g, 51%). ¹H NMR (400 MHz, DMSO-*d*₆) δ 12.88 (s, 1H), 8.41 (s, 1H), 8.20 (t, *J* = 8.3 Hz, 2H), 7.96 – 7.86 (m, 2H), 7.77 (d, *J* = 8.2 Hz, 1H), 7.60 (dq, *J* = 15.3, 7.2 Hz, 3H). MS (ESI + APCI) *m/z*: 432.9 [M+H]⁺.

2-(4-Oxo-3,4-dihydroquinazolin-2-yl) benzofuran-3-carbaldehyde (f). The compound **e** (196 mg, 0.45 mmol) was dissolved in DMSO (4 mL) then was heated at 100 °C for 2 h. Next, the mixture was poured into ice-water, filtered, and desiccated under vacuum to give the crude product, which was then purified by using column chromatography with dichloromethane/petroleum ether, resulting in a yellow solid (80 mg, 60%). ¹H NMR (400 MHz, DMSO-*d*₆) δ 13.07 (s, 1H), 10.98 (s, 1H), 8.22 (t, *J* = 7.0 Hz, 2H), 7.90 (t, *J* = 9.3 Hz, 2H), 7.81 (d, *J* = 8.1 Hz, 1H), 7.62 (q, *J* = 7.6 Hz, 2H), 7.55 – 7.49 (m, 1H). MS (ESI + APCI) *m/z*: 291.1 [M+H]⁺.

2-(4-Chloroquinazolin-2-yl) benzofuran-3-carbaldehyde (g). The compound **f** (0.2 g, 0.68 mmol) dissolving in POCl₃ (3 mL) was heated at 60 °C for 2 h. Next, the mixture was poured into ice-water and extracted with dichloromethane. The combined organic layers were dried over anhydrous Na₂SO₄, filtered, and concentrated under reduced pressure. The crude product was purified by using column chromatography with dichloromethane/petroleum ether, resulting in a pale yellow solid (30 mg, 14%). ¹H NMR (400 MHz, CDCl₃) δ 8.71 (s, 1H), 8.32 (d, *J* = 9.1 Hz, 1H), 8.26 (d, *J* = 7.8 Hz, 1H), 8.22 (d, *J* = 8.5 Hz, 1H), 8.03 (t, *J* = 8.4 Hz, 1H), 7.78 (t, *J* = 7.7 Hz, 1H), 7.73 (d, *J* = 8.3 Hz, 1H), 7.50 (t, *J* = 7.8 Hz, 1H), 7.42 (t, *J* = 7.5 Hz, 1H). MS (ESI + APCI) *m/z*: 309.0 [M+H]⁺.

The compound **h** was prepared by 2-aminobenzamide according to our preliminary literature procedure [17].

General method A for the preparation of the compounds i-j. To a solution of compound **h** dissolving in DMF was added KOH (1.2 eq) and iodomethane (1.2 eq) or benzyl bromide (1.6 eq). After being stirred for 2 h, the reaction was quenched with water and extracted with dichloromethane. The combined organic layers were dried over anhydrous Na₂SO₄, filtered, and concentrated under reduced pressure. The crude product was purified by using column chromatography to give the desired product.

General method B for the preparation of the compounds m-n, s. To a stirred suspension of carboxylic acid **k**, **l** or **q** in dry dichloromethane was added acyl chloride (3 eq) and two drops of DMF, and the mixture was stirred at room temperature for 2 h. Next, the acyl chloride was removed by using a rotary evaporator. The residue was dissolved in *tert*-butanol, then anthranilamide (1 eq) and potassium *tert*-butoxide (2 eq) were added, and it was heated at 100 °C for 8 h. The solution was poured into ice-water, and the pH was adjusted to 7.0. The residue was filtered, washed with water, and desiccated under vacuum to give the crude product, which was then purified by using column chromatography to give the desired product.

General method C for the preparation of the compounds o-p. Vilsmeier reagent was prepared by the reaction of phosphorus oxychloride with N, N-dimethylformamide at the volume ratio of 2:1 in an ice bath for 0.5 h. **m** or **n** was slowly added to Vilsmeier reagent and reacted at room temperature for 1 h. Next, the reaction solution was slowly dripped into the ice water and neutralized with 10% NaOH to give the product. The crude product was purified by using column chromatography to give the desired product.

The compound **r** was prepared by 2-aminobenzamide according to preliminary literature procedure [18].

General method D for the preparation of the compounds t-v. The compound **d**, **r-s** dissolving in excess POCl₃ was heated at 50 ~ 80 °C for 6 ~ 10 h. The solution was poured into ice-water, and pH was adjusted to 7.0 by saturated solution of NaHCO₃. The residue was filtered, washed with water, and desiccated under vacuum to give the crude product, which was purified by using column chromatography to give the desired product.

4-Chloro-2-(1-methyl-1H-indol-2-yl)quinazoline (i). Following general method A, the compound **i** was obtained from **h** (0.50 g, 1.79 mmol) as a yellow solid (136 mg, 27%). ¹H NMR (400 MHz, CDCl₃) δ 8.27 (d, *J* = 8.3 Hz, 1H), 8.10 (d, *J* = 8.5 Hz, 1H), 7.95 (t, *J* = 7.0 Hz, 1H), 7.83 – 7.71 (m, 2H), 7.71 – 7.64 (m, 1H), 7.46 (d, *J* = 8.4 Hz, 1H), 7.39 – 7.33 (m, 1H), 7.18 (t, *J* = 7.4 Hz, 1H), 4.40 (s, 3H). MS (ESI + APCI) *m/z*: 294.1[M+H]⁺.

2-(1-Benzyl-1H-indol-2-yl)-4-chloroquinazoline (j). Following general method A, the compound **j** was obtained from **h** (200 mg, 0.72 mmol) as a pale red solid (200 mg, 76%). ¹H NMR (400 MHz, CDCl₃) δ 8.21 (d, *J* = 8.3 Hz, 1H), 7.89 (dd, *J* = 18.2, 8.9 Hz, 3H), 7.78 (d, *J* = 7.8 Hz, 1H), 7.62 (t, *J* = 6.8 Hz, 1H), 7.42 (d, *J* = 8.2 Hz, 1H), 7.36 – 7.27 (m, 2H), 7.24 (d, *J* = 6.9 Hz, 1H), 7.21 (s, 1H), 7.19 (s, 1H), 7.18 – 7.11 (m, 2H), 6.30 (s, 2H). MS (ESI + APCI) *m/z*: 370.1[M+H]⁺.

2-(1H-Indol-2-yl)quinazolin-4(3H)-one (m). Following general method B, the compound **m** was obtained from **k** (500 mg, 3.11 mmol) as a white solid (0.63 g, 78%). ¹H NMR (400 MHz, DMSO-*d*₆) δ 12.61 (s, 1H), 11.80 (s, 1H), 8.16 (dd, *J* = 7.9, 1.0 Hz, 1H), 7.88 – 7.83 (m, 1H), 7.75 (d, *J* = 7.9 Hz, 1H), 7.67 (d, *J* = 1.5 Hz, 1H), 7.65 (d, *J* = 8.0 Hz, 1H), 7.56 – 7.48 (m, 2H), 7.26 – 7.21 (m, 1H), 7.07 (t, *J* = 7.2 Hz, 1H); MS (ESI + APCI) *m/z*: 262.1[M+H]⁺.

2-(5-Methoxy-1H-indol-2-yl)quinazolin-4(3H)-one (n). Following general method B, the compound **n** was obtained from **l** (0.96 g, 5 mmol) as a yellow solid (1.02 g, 70%). ¹H NMR (400 MHz, DMSO-*d*₆) δ 12.56 (s, 1H), 11.64 (s, 1H), 8.16 (d, *J* = 7.4 Hz, 1H), 7.84 (t, *J* = 7.1 Hz, 1H), 7.73 (d, *J* = 7.9 Hz, 1H), 7.59 (s, 1H), 7.50 (t, *J* = 7.2 Hz, 1H), 7.43 (d, *J* = 8.8 Hz, 1H), 7.11 (s, 1H), 6.89 (d, *J* = 7.9 Hz, 1H), 3.79 (s, 3H). MS (ESI + APCI) *m/z*: 292.1[M+H]⁺.

2-(4-Chloroquinazolin-2-yl)-1H-indole-3-carbaldehyde (o). Following general method C, the compound **o** was obtained from **m** (100 mg, 0.38 mmol) as a pale yellow solid (113 mg, 97%). ¹H NMR (400 MHz, DMSO-*d*₆) δ 12.79 (s, 1H), 11.22 (s, 1H), 8.35 (d, *J* = 8.1 Hz, 1H), 8.30 (d, *J* = 7.8 Hz, 1H), 8.20 (q, *J* = 8.0 Hz, 2H), 7.93 (t, *J* = 6.8 Hz, 1H), 7.67 (d, *J* = 8.0 Hz, 1H), 7.36 (t, *J* = 7.5 Hz, 1H), 7.28 (t, *J* = 7.3 Hz, 1H). ¹³C NMR (101 MHz, DMSO-*d*₆) δ 189.6, 162.3, 153.7, 151.2, 140.4, 136.9, 136.7, 130.6, 129.0, 126.5, 126.3, 125.6, 123.6, 122.6, 122.6, 117.7, 113.5. MS (ESI + APCI) *m/z*: 308.2[M+H]⁺.

2-(4-Chloroquinazolin-2-yl)-5-methoxy-1H-indole-3-carbaldehyde (p). Following general method C, the compound **p** was obtained from **n** (1 g, 3.13 mmol) as a yellow solid (0.87 g, 75%). ¹H NMR (400 MHz, DMSO-*d*₆) δ 12.70 (s, 1H), 11.20 (s, 1H), 8.34 (d, *J* = 8.2 Hz, 1H), 8.24 – 8.14 (m, 2H), 7.91 (t, *J* = 6.1 Hz, 1H), 7.78 (d, *J* = 2.2 Hz, 1H), 7.57 (d, *J* = 8.9 Hz, 1H), 6.99 (d, *J* = 2.5 Hz, 1H), 3.83 (s, 3H). Purity: 99.1% by HPLC. HRMS (ESI + APCI) *m/z*: calcd for C₁₈H₁₂N₃O₂Cl, [M+H]⁺ 338.0691, found 338.0694.

2-(3-Methylbenzo[b]thiophen-2-yl)quinazolin-4(3H)-one (s). Following general method B, the compound **s** was obtained from **q** (8 g, 41.7 mmol) as a white solid (5.3 g, 43%). ¹H NMR (400 MHz, DMSO-*d*₆) δ 12.49 (s, 1H), 8.18 (d, *J* = 7.8 Hz, 1H), 8.08 – 8.02 (m, 1H), 7.97 – 7.91 (m, 1H), 7.86 (t, *J* = 7.6 Hz, 1H), 7.73 (d, *J* = 8.0 Hz, 1H), 7.56 (t, *J* = 7.5 Hz, 1H), 7.52 (d, *J* = 3.1 Hz, 1H), 7.51

(d, $J = 3.3$ Hz, 1H), 2.65 (s, 3H). MS (ESI + APCI) m/z : 293.1[M+H]⁺.

4-Chloro-2-(3-methylbenzofuran-2-yl) quinazoline (t). Following general method D, the compound **t** was obtained from **d** (1 g, 3.13 mmol) at 50 °C for 10 h, resulting in a yellow solid (0.68 g, 64%). ¹H NMR (400 MHz, DMSO-*d*₆) δ 7.73 (d, $J = 7.6$ Hz, 2H), 7.69 (d, $J = 7.2$ Hz, 1H), 7.65 – 7.58 (m, 2H), 7.46 – 7.41 (m, 1H), 7.39 (t, $J = 7.5$ Hz, 1H), 7.34 (t, $J = 7.4$ Hz, 1H), 2.75 (s, 3H). MS (ESI + APCI) m/z : 295.1 [M+H]⁺.

4-Chloro-2-(3-methyl-1H-indol-2-yl) quinazoline (u). Following general method D, the compound **u** was obtained from **r** (60 mg, 0.22 mmol) with two drops DMF at 80 °C for 6 h, resulting in a pale yellow solid (50 mg, 78%). ¹H NMR (400 MHz, CDCl₃) δ 9.39 (s, 1H), 8.22 (d, $J = 8.3$ Hz, 1H), 8.02 (d, $J = 8.4$ Hz, 1H), 7.97 – 7.88 (m, 1H), 7.72 (d, $J = 8.0$ Hz, 1H), 7.62 (t, 1H), 7.43 (d, $J = 8.2$ Hz, 1H), 7.32 (t, $J = 8.1$ Hz, 1H), 7.16 (t, $J = 7.9$ Hz, 1H), 2.94 (s, 3H). MS (ESI) m/z 294.1 [M+H]⁺.

*4-Chloro-2-(3-methylbenzo[*b*]thiophen-2-yl) quinazoline (v)*. Following general method D, the compound **v** was obtained from **s** (1 g, 3.42 mmol) with two drops DMF at 80 °C for 6 h, resulting in a white solid (0.91 g, 86%). ¹H NMR (400 MHz, CDCl₃) δ 8.12 (d, $J = 8.3$ Hz, 1H), 7.97 (d, $J = 8.4$ Hz, 1H), 7.83 (d, $J = 8.3$ Hz, 1H), 7.81 – 7.74 (m, 2H), 7.54 (t, $J = 7.6$ Hz, 1H), 7.35 – 7.29 (m, 2H), 2.96 (s, 3H). MS (ESI) m/z : 311.0[M+H]⁺.

General method E for the preparation of the target compounds 1-5 (series I) A mixture of intermediate **g** (30 mg, 0.1 mmol), triethylamine (30 μ L), and the respective amine (1 mmol) in toluene (10 mL) was heated at 80 °C for 1 h. Next, most of the toluene was removed by using a rotary evaporator. The crude product was purified via flash chromatography to give the desired product.

General method F for the preparation of the target compounds 6-7 (series I) A mixture of

intermediate **i** or **j** (100 mg), triethylamine (30 μ L), and the respective amine (1 mmol) in toluene (1 mL) was stirred for 1 h. Next, most of the toluene was removed by using a rotary evaporator, then dissolved it in the prepared Vilsmeier reagents. Next, the mixture solution was poured into ice-water and be well stirred, then the pH was adjusted to 7~8, filtered, and desiccated under vacuum to give the crude product, which was purified via flash chromatography to give the desired product.

General method G for the preparation of the target compounds 8-9 (series II) To a solution of the respective thiol chain (3.3 mmol) in DMF (5 mL) were added sodium hydride (72 mg, 3 mmol). Until the solution changed from colorless clarification to white turbidity, the compound **o** (100 mg, 0.33 mmol) was added and the reaction was heated at 90 °C for 8 h. Next, the mixture solution was poured into ice-water and be well stirred, then the pH was adjusted to 7, filtered, and desiccated under vacuum to give the crude product, which was purified by column chromatography to give the desired product.

General method H for the preparation of the target compounds 10-12 (series II) To a solution of **o** (100 mg, 0.33 mmol) in DMF (5 mL) were added K_2CO_3 (91 mg, 0.66 mmol) and the respective amine (3.3 mmol). After being stirred for 1~4 h, the reaction was quenched with water, then the pH value was adjusted to 8, filtered, and desiccated under vacuum to give the crude product, which was purified by column chromatography to give the desired product.

General method I for the preparation of the target compounds 13-17 (series II) and 31-35 (series IV) A solution of the respective alcohol chain (1 mmol) in tetrahydrofuran (4 mL) was added sodium hydride (24 mg, 1 mmol). Until no bubbles were bubbled up, the compound **o** (59 mg, 0.2 mmol) or **t** (59 mg, 0.2 mmol) was added and the reaction was stirred at room temperature for 1 h. Next, most of the tetrahydrofuran was removed by using a rotary evaporator. The residual solution was poured into

ice-water and be well stirred, filtered, and desiccated under vacuum to give the crude product, which was purified by column chromatography to give the desired product.

General method J for the preparation of the target compounds 18-23 (series III) A mixture of intermediate **p** (150 mg, 0.44 mmol), triethylamine (30 μ L), and the respective amine (4.4 mmol) in toluene (5 mL) was heated at 60 °C for 6 h. Next, the mixture solution was poured into ice-water and be well stirred, then the pH was adjusted to 7~8, filtered, and desiccated under vacuum to give the crude product, which was purified via flash chromatography to give the desired product.

General method K for the preparation of the target compounds 24-30 (series IV) A mixture of intermediate **u** (100 mg, 0.34 mmol), triethylamine (30 μ L), and the respective amine (2.5 mmol) in toluene (5 mL) was heated at 80 °C for 6 h. Next, the mixture solution was poured into ice-water and well stirred, then the pH was adjusted to 9, filtered, and desiccated under vacuum to give the crude product, which was then purified via flash chromatography on a silica gel to give the desired product.

General method L for the preparation of the target compounds 36-40 (series IV) A mixture of intermediate **v** (100 mg, 0.32 mmol), triethylamine (30 μ L), and the respective amine (3.2 mmol) in toluene (5 mL) was heated under 25 ~ 60 °C for 2 h. Next, the mixture solution was poured into ice-water and be well stirred, then the pH was adjusted to 7, filtered, and desiccated under vacuum to give the crude product, which was purified via flash chromatography to give the desired product.

2-(4-((2-(Dimethylamino)ethyl)amino)quinazolin-2-yl)benzofuran-3-carbaldehyde (1). Following general method E, the compound **1** was obtained from **g** and *N,N*-dimethylethane-1,2-diamine as a pale yellow solid (21 mg, 59%): m.p. 124.8-126.0 °C; ^1H NMR (400 MHz, CDCl_3) δ 11.40 (s, 1H), 8.42 (d, $J = 8.5$ Hz, 1H), 8.35 (d, $J = 7.2$ Hz, 1H), 8.04 (d, $J = 8.1$ Hz, 1H), 7.83 (t, $J = 7.8$ Hz, 1H), 7.71 (d, $J = 7.7$ Hz, 1H), 7.66 – 7.58 (m, 1H), 7.49 – 7.43 (m 1H), 7.43 – 7.37 (m, 1H), 4.13 (br, 2H),

3.35 (br, 2H), 2.86 (s, 6H). ^{13}C NMR (101 MHz, DMSO- d_6) δ 190.6, 160.3, 160.0, 153.8, 153.0, 149.4, 134.1, 128.7, 127.7 (2C), 125.7, 125.2, 123.9, 123.1, 120.8, 115.0, 112.4, 56.1, 43.5 (2C), 37.3. Purity: 98.5% by HPLC. HRMS (ESI) m/z : calcd for $\text{C}_{21}\text{H}_{20}\text{N}_4\text{O}_2$, $[\text{M}+\text{H}]^+$ 361.1659, found 361.1649.

2-(4-((3-(Dimethylamino)propyl)amino)quinazolin-2-yl)benzofuran-3-carbaldehyde (2).

Following general method E, the compound **2** was obtained from **g** and *N,N*-dimethylpropane-1,3-diamine as a pale yellow solid (26 mg, 70%): m.p. 99.4-102.1 °C; ^1H NMR (400 MHz, CDCl_3) δ 11.48 (s, 1H), 8.95 (s, 1H), 8.36 (d, $J = 7.5$ Hz, 1H), 8.04 (d, $J = 8.3$ Hz, 1H), 8.00 (d, $J = 7.9$ Hz, 1H), 7.80 (t, $J = 7.6$ Hz, 1H), 7.72 (d, $J = 8.2$ Hz, 1H), 7.56 (t, $J = 7.6$ Hz, 1H), 7.48 – 7.43 (m, 1H), 7.40 (t, $J = 7.4$ Hz, 1H), 3.88 (q, $J = 5.1$ Hz, 2H), 2.95 – 2.91 (m, 2H), 2.65 (s, 6H), 2.18 – 2.11 (m, 2H). ^{13}C NMR (101 MHz, DMSO- d_6) δ 190.8, 160.1, 160.1, 153.8, 153.2, 149.4, 133.9, 128.7, 127.6 (2C), 125.7, 125.3, 123.5, 123.1, 120.8, 114.9, 112.4, 56.3, 44.2 (2C), 40.2, 25.2. Purity: 99.8% by HPLC. HRMS (ESI) m/z : calcd for $\text{C}_{22}\text{H}_{22}\text{N}_4\text{O}_2$, $[\text{M}+\text{H}]^+$ 375.1816, found 375.1807.

2-(4-((4-(Dimethylamino)butyl)amino)quinazolin-2-yl)benzofuran-3-carbaldehyde (3). Following general method E, the compound **3** was obtained from **g** and *N,N*-dimethylbutane-1,4-diamine as a yellow solid (22 mg, 58%): m.p. 121.6-123.9 °C; ^1H NMR (400 MHz, CDCl_3) δ 11.50 (s, 1H), 8.37 (d, $J = 7.1$ Hz, 2H), 8.03 (t, $J = 9.4$ Hz, 2H), 7.79 (t, $J = 7.5$ Hz, 1H), 7.73 (d, $J = 8.0$ Hz, 1H), 7.54 (t, $J = 7.5$ Hz, 1H), 7.48 – 7.37 (m, 2H), 3.72 (q, $J = 5.2$ Hz, 2H), 2.66 (t, $J = 6.0$ Hz, 2H), 2.50 (s, 6H), 2.01 – 1.91 (m, 2H), 1.90 – 1.82 (m, 2H). ^{13}C NMR (101 MHz, CDCl_3) δ 191.3, 159.9, 159.8, 154.2, 153.6, 149.5, 133.0, 129.0, 126.9, 126.8, 125.5, 124.9, 123.4, 121.9, 121.5, 114.8, 112.0, 58.8, 44.9 (2C), 41.6, 26.3, 24.8. Purity: 99.8% by HPLC. HRMS (ESI) m/z : calcd for $\text{C}_{23}\text{H}_{24}\text{N}_4\text{O}_2$, $[\text{M}+\text{H}]^+$ 389.1972, found 389.1962.

2-(4-((2-(Pyrrolidin-1-yl)ethyl)amino)quinazolin-2-yl)benzofuran-3-carbaldehyde (4). Following general method E, the compound **4** was obtained from **g** and 2-(pyrrolidin-1-yl)ethanamine as a pale yellow solid (23 mg, 61%): m.p. 139.9-141.4 °C; ¹H NMR (400 MHz, CDCl₃) δ 11.46 (s, 1H), 8.37 (d, *J* = 7.5 Hz, 1H), 8.15 (d, *J* = 6.9 Hz, 1H), 8.06 (d, *J* = 8.3 Hz, 1H), 7.86 – 7.80 (m, 1H), 7.72 (d, *J* = 8.1 Hz, 1H), 7.61 (t, *J* = 7.5 Hz, 1H), 7.49 – 7.44 (m, 1H), 7.42 (t, *J* = 7.6 Hz, 1H), 3.96 (br, 2H), 3.19 (br, 2H), 3.01 (br, 4H), 2.03 (br, 4H). ¹³C NMR (101 MHz, CDCl₃) δ 190.8, 159.7, 159.6, 154.2, 153.2, 149.5, 133.4, 129.1, 127.5, 126.9, 125.4, 125.0, 123.4, 122.2, 121.5, 114.6, 112.0, 54.5, 54.2 (2C), 39.1, 23.5 (2C). Purity: 99.6% by HPLC. HRMS (ESI) *m/z*: calcd for C₂₃H₂₂N₄O₂, [M+H]⁺387.1816, found 387.1806.

2-(4-((3-(Pyrrolidin-1-yl)propyl)amino)quinazolin-2-yl)benzofuran-3-carbaldehyde (5). Following general method E, the compound **5** was obtained from **g** and 3-(pyrrolidin-1-yl)propan-1-amine as a yellow solid (24 mg, 61%): m.p. 90.7-92.0 °C; ¹H NMR (400 MHz, MeOD-*d*₄) δ 11.39 (s, 1H), 8.28 (d, *J* = 7.8 Hz, 1H), 8.11 (d, *J* = 8.2 Hz, 1H), 7.95 (d, *J* = 8.4 Hz, 1H), 7.87 (t, *J* = 7.3 Hz, 1H), 7.71 (d, *J* = 8.3 Hz, 1H), 7.62 (t, *J* = 8.0 Hz, 1H), 7.53 (t, *J* = 7.7 Hz, 1H), 7.44 (t, *J* = 7.5 Hz, 1H), 3.75 (t, *J* = 7.0 Hz, 2H), 2.91 – 2.79 (m, 6H), 2.14 – 2.05 (m, 2H), 1.91 (br, 4H). ¹³C NMR (101 MHz, CDCl₃) δ 191.3, 159.9, 159.8, 154.2, 153.7, 149.4, 133.0, 129.1, 126.9, 126.8, 125.5, 124.9, 123.4, 121.8, 121.5, 115.0, 112.0, 55.4, 54.1 (2C), 29.7, 24.8, 23.5 (2C). Purity: 99.7% by HPLC. HRMS (ESI) *m/z*: calcd for C₂₄H₂₄N₄O₂, [M+H]⁺401.1972, found 401.1961.

2-(4-((3-(Dimethylamino)propyl)amino)quinazolin-2-yl)-1-methyl-1H-indole-3-carbaldehyde (6). Following general method F, the compound **6** was obtained from **i** and *N,N*-dimethylpropane-1,3-diamine as a pale yellow solid (43 mg, 47%): m.p. 108.1-108.9 °C; ¹H NMR (400 MHz, DMSO-*d*₆) δ 10.41 (s, 1H), 8.74 (t, *J* = 5.0 Hz, 1H), 8.32 (d, *J* = 8.2 Hz, 1H), 8.29

(d, $J = 7.9$ Hz, 1H), 7.90 – 7.81 (m, 2H), 7.72 (d, $J = 8.2$ Hz, 1H), 7.66 – 7.59 (m, 1H), 7.41 (t, $J = 7.4$ Hz, 1H), 7.33 (t, $J = 7.4$ Hz, 1H), 4.10 (s, 3H), 3.63 (q, $J = 6.3$ Hz, 2H), 2.38 (t, $J = 6.5$ Hz, 2H), 2.18 (s, 6H), 1.89 – 1.79 (m, 2H). ^{13}C NMR (101 MHz, DMSO- d_6) δ 188.4, 159.9, 154.6, 149.5, 147.5, 137.7, 133.6, 128.5, 127.2, 124.9, 124.7, 123.5, 123.3, 122.0, 116.3, 114.2, 111.6, 57.2, 45.4 (2C), 39.7, 32.7, 26.7. Purity: 99.3% by HPLC. HRMS (ESI) m/z : calcd for $\text{C}_{23}\text{H}_{25}\text{N}_5\text{O}$, $[\text{M}+\text{H}]^+$ 388.2132, found 388.2122.

Benzyl-2-(4-((3-(dimethylamino)propyl)amino)quinazolin-2-yl)-1H-indole-3-carbaldehyde (7).

Following general method F, the compound **7** was obtained from **j** and N,N-dimethylpropane-1,3-diamine as a pale yellow solid (68 mg, 54%): m.p.119.0-119.9 °C; ^1H NMR (400 MHz, DMSO- d_6) δ 10.47 (s, 1H), 8.65 (t, $J = 5.0$ Hz, 1H), 8.34 – 8.23 (m, 2H), 7.87 – 7.81 (m, 1H), 7.79 (d, $J = 8.0$ Hz, 1H), 7.61 (t, $J = 7.4$ Hz, 1H), 7.56 (d, $J = 8.3$ Hz, 1H), 7.35 – 7.26 (m, 2H), 7.23 (t, $J = 7.1$ Hz, 2H), 7.19 (d, $J = 6.8$ Hz, 1H), 7.13 (d, $J = 7.5$ Hz, 2H), 6.03 (s, 2H), 3.46 (q, $J = 6.5$ Hz, 2H), 2.20 (t, $J = 6.9$ Hz, 2H), 2.11 (s, 6H), 1.71 – 1.63 (m, 2H). ^{13}C NMR (101 MHz, DMSO- d_6) δ 188.7, 159.8, 154.5, 149.4, 147.1, 138.0, 137.1, 133.6, 128.8 (2C), 128.4, 127.6, 127.1, 127.0 (2C), 125.2, 124.8, 123.5, 123.2, 122.1, 116.8, 114.1, 112.1, 57.3, 48.1, 45.4 (2C), 39.6, 26.8. Purity: 99.8% by HPLC. HRMS (ESI) m/z : calcd for $\text{C}_{29}\text{H}_{29}\text{N}_5\text{O}$, $[\text{M}+\text{H}]^+$ 464.2445, found 464.2437.

2-(4-((2-(Dimethylamino)ethyl)thio)quinazolin-2-yl)-1H-indole-3-carbaldehyde (8). Following general method G, the compound **8** was obtained from **o** and 2-(dimethylamino)ethane-1-thiol as a yellow solid (114 mg, 92%): m.p.178.9-179.5 °C; ^1H NMR (400 MHz, CDCl_3) δ 11.57 (s, 1H), 11.47 (s, 1H), 8.52 (d, $J = 7.4$ Hz, 1H), 8.01 (d, $J = 8.2$ Hz, 1H), 7.95 (d, $J = 8.4$ Hz, 1H), 7.84 (t, $J = 7.7$ Hz, 1H), 7.54 (t, $J = 7.6$ Hz, 1H), 7.40 (d, $J = 7.6$ Hz, 1H), 7.36 – 7.27 (m, 2H), 3.47 (t, $J = 6.7$ Hz,

2H), 2.75 (t, $J = 6.7$ Hz, 2H), 2.41 (s, 6H). ^{13}C NMR (101 MHz, CDCl_3) δ 190.4, 171.2, 153.0, 148.4, 141.6, 135.7, 134.3, 129.2, 127.7, 127.1, 125.1, 123.9, 123.5, 123.2, 122.7, 118.0, 111.6, 59.1, 45.3 (2C), 28.9. Purity: 99.5% by HPLC. HRMS (ESI) m/z : calcd for $\text{C}_{21}\text{H}_{20}\text{N}_4\text{OS}$, $[\text{M}+\text{H}]^+$ 377.1431, found 377.1434.

2-(4-((2-(Diethylamino)ethyl)thio)quinazolin-2-yl)-1H-indole-3-carbaldehyde (**9**). Following general method G, the compound **9** was obtained from **o** and 2-(diethylamino)ethane-1-thiol as a yellow solid (75 mg, 56%): m.p.113.8-114.2 °C; ^1H NMR (400 MHz, $\text{DMSO}-d_6$) δ 12.54 (s, 1H), 11.21 (s, 1H), 8.32 (d, $J = 7.9$ Hz, 1H), 8.20 (d, $J = 8.2$ Hz, 1H), 8.13 – 8.01 (m, 2H), 7.76 (t, $J = 7.0$ Hz, 1H), 7.68 (d, $J = 8.1$ Hz, 1H), 7.37 (t, $J = 7.5$ Hz, 1H), 7.28 (t, $J = 7.4$ Hz, 1H), 3.67 (t, $J = 5.7$ Hz, 2H), 2.82 (br, 2H), 2.64 – 2.53 (m, 4H), 0.94 (t, $J = 6.9$ Hz, 6H). ^{13}C NMR (101 MHz, $\text{DMSO}-d_6$) δ 189.5, 172.4, 153.3, 147.9, 142.2, 136.4, 135.4, 129.1, 128.9, 126.6, 125.3, 124.3, 123.3, 122.6, 122.4, 117.3, 113.3, 51.5, 46.6 (2C), 28.2, 12.0 (2C). Purity: 98.4% by HPLC. HRMS (ESI) m/z : calcd for $\text{C}_{23}\text{H}_{24}\text{N}_4\text{OS}$, $[\text{M}+\text{H}]^+$ 405.1744, found 405.1757.

2-(4-((3-(Pyrrolidin-1-yl)propyl)amino)quinazolin-2-yl)-1H-indole-3-carbaldehyde (**10**).

Following general method H, the compound **10** was obtained from **o** and 3-(pyrrolidin-1-yl)propan-1-amine as a golden solid (81 mg, 62%): m.p.176.9-177.3 °C; ^1H NMR (400 MHz, CDCl_3) δ 11.36 (s, 1H), 10.44 (s, 1H), 9.12 (s, 1H), 8.42 (d, $J = 4.6$ Hz, 1H), 7.65 (d, $J = 8.2$ Hz, 1H), 7.54 (t, $J = 7.5$ Hz, 1H), 7.47 (d, $J = 8.0$ Hz, 1H), 7.25 (t, $J = 7.0$ Hz, 2H), 7.18 (d, $J = 5.2$ Hz, 2H), 3.62 (d, $J = 3.4$ Hz, 2H), 2.69 (t, $J = 6.8$ Hz, 2H), 2.56 (br, 4H), 1.82 (br, 4H), 1.79 – 1.73 (m, 2H). ^{13}C NMR (101 MHz, CDCl_3) δ 190.2, 158.6, 153.6, 148.2, 142.0, 133.9, 131.6, 127.1, 126.0, 124.8, 123.7, 122.2, 121.8, 120.4, 116.5, 113.6, 110.4, 55.2, 53.1 (2C), 42.1, 24.1, 22.6 (2C). Purity: 99.7% by HPLC. HRMS (ESI) m/z : calcd for $\text{C}_{24}\text{H}_{25}\text{N}_5\text{O}$, $[\text{M}+\text{H}]^+$ 400.2132, found 400.2126.

2-(4-((4-(Pyrrolidin-1-yl)butyl)amino)quinazolin-2-yl)-1H-indole-3-carbaldehyde (11). Following general method H, the compound **11** was obtained from **o** and 4-(pyrrolidin-1-yl)butan-1-amine as a yellow green solid (22 mg, 16%): m.p.83.6-84.1 °C; ¹H NMR (400 MHz, DMSO-*d*₆) δ 12.33 (s, 1H), 11.33 (s, 1H), 8.58 (t, *J* = 4.8 Hz, 1H), 8.31 (t, *J* = 8.2 Hz, 2H), 7.88 – 7.80 (m, 2H), 7.67 (d, *J* = 8.1 Hz, 1H), 7.56 (t, *J* = 5.7 Hz, 1H), 7.31 (t, *J* = 7.5 Hz, 1H), 7.24 (t, *J* = 7.4 Hz, 1H), 3.68 (q, *J* = 5.8 Hz, 2H), 2.48 – 2.38 (m, 6H), 1.78 – 1.71 (m, 2H), 1.65 – 1.60 (m, 4H), 1.60 – 1.47 (m, 2H). ¹³C NMR (101 MHz, DMSO-*d*₆) δ 190.2, 160.1, 154.9, 149.6, 143.8, 136.1, 133.6, 128.2, 126.7, 126.7, 124.8, 123.4, 123.0, 122.4, 116.9, 114.6, 113.2, 55.7, 53.9 (2C), 41.3, 27.0, 26.3, 23.5 (2C). Purity: 99.6% by HPLC. HRMS (ESI) *m/z*: calcd for C₂₅H₂₇N₅O, [M+H]⁺ 414.2288, found 414.2273.

2-(4-((4-(Diethylamino)butyl)amino)quinazolin-2-yl)-1H-indole-3-carbaldehyde (12). Following general method H, the compound **12** was obtained from **o** and *N,N*-diethylbutane-1,4-diamine as a golden solid (90 mg, 66%): m.p.122.9-123.7 °C; ¹H NMR (400 MHz, CDCl₃) δ 11.38 (s, 1H), 10.29 (s, 1H), 8.45 (d, *J* = 6.2 Hz, 1H), 7.82 (d, *J* = 7.5 Hz, 1H), 7.73 (d, *J* = 7.8 Hz, 1H), 7.63 (t, *J* = 7.5 Hz, 1H), 7.52 (br, 1H), 7.36 (br, 2H), 7.28 – 7.17 (m, 2H), 3.61 (br, 2H), 3.12 – 2.82 (m, 2H), 2.68 – 2.52 (m, 4H), 1.76 (br, 2H), 1.70 – 1.61 (m, 2H), 1.03 (t, *J* = 6.3 Hz, 6H). ¹³C NMR (101 MHz, CDCl₃) δ 190.0, 158.7, 153.4, 148.4, 141.9, 133.9, 131.9, 127.2, 126.0, 125.1, 123.9, 122.3, 122.0, 120.8, 116.5, 113.4, 110.4, 51.0, 45.6 (2C), 40.6, 25.6, 23.6, 9.4 (2C). Purity: 99.8% by HPLC. HRMS (ESI) *m/z*: calcd for C₂₅H₂₉N₅O, [M+H]⁺ 416.1445, found 416.2442.

2-(4-(2-(Dimethylamino)ethoxy)quinazolin-2-yl)-1H-indole-3-carbaldehyde (13). Following general method I, the compound **13** was obtained from **o** and 2-(dimethylamino)ethan-1-ol as a pale yellow solid (50 mg, 72%): m.p. 176.6-177.9 °C; ¹H NMR (400 MHz, CDCl₃) δ 11.42 (s, 1H), 10.18 (s, 1H), 8.53 (d, *J* = 7.8 Hz, 1H), 8.17 (d, *J* = 8.2 Hz, 1H), 7.95 (d, *J* = 8.2 Hz, 1H), 7.89 – 7.81 (m,

1H), 7.60 – 7.52 (m, 1H), 7.50 (d, $J = 7.9$ Hz, 1H), 7.41 – 7.34 (m, 1H), 7.34 – 7.28 (m, 1H), 4.77 (t, $J = 5.5$ Hz, 2H), 2.93 (t, $J = 5.5$ Hz, 2H), 2.44 (s, 6H). ^{13}C NMR (101 MHz, CDCl_3) δ 190.1, 166.7, 153.4, 151.0, 141.1, 135.2, 134.3, 127.6, 127.5, 127.0, 125.34, 123.8, 123.5, 123.3, 118.0, 115.5, 111.4, 65.9, 57.7, 46.0 (2C). Purity: 99.9% by HPLC. HRMS (ESI) m/z : calcd for $\text{C}_{21}\text{H}_{20}\text{N}_4\text{O}_2$, $[\text{M}+\text{H}]^+$ 361.1659, found 361.1657.

2-(4-(3-(Dimethylamino)propoxy)quinazolin-2-yl)-1H-indole-3-carbaldehyde (**14**). Following general method I, the compound **14** was obtained from **o** and 3-(dimethylamino)propan-1-ol as a pale yellow solid (61 mg, 80%): m.p. 199.9-201.5 °C; ^1H NMR (400 MHz, CDCl_3) δ 11.46 (s, 1H), 10.26 (s, 1H), 8.54 (d, $J = 7.6$ Hz, 1H), 8.20 (d, $J = 8.1$ Hz, 1H), 7.98 (d, $J = 8.3$ Hz, 1H), 7.89 (t, $J = 7.7$ Hz, 1H), 7.60 (t, $J = 7.3$ Hz, 1H), 7.54 (d, $J = 8.1$ Hz, 1H), 7.38 (t, $J = 7.0$ Hz, 1H), 7.33 (t, $J = 7.5$ Hz, 1H), 4.78 (t, $J = 6.4$ Hz, 2H), 2.61 (t, $J = 7.1$ Hz, 2H), 2.35 (s, 6H), 2.23 – 2.13 (m, 2H). ^{13}C NMR (101 MHz, $\text{DMSO}-d_6$) δ 189.8, 166.8, 154.0, 151.1, 142.0, 136.4, 135.4, 128.6, 128.1, 126.6, 125.3, 124.2, 123.4, 122.6, 117.3, 115.4, 113.4, 65.8, 55.1, 43.8 (2C), 25.1. Purity: 99.9% by HPLC. HRMS (ESI) m/z : calcd for $\text{C}_{22}\text{H}_{22}\text{N}_4\text{O}_2$, $[\text{M}+\text{H}]^+$ 375.1816, found 375.1813.

2-(4-(4-(Dimethylamino)butoxy)quinazolin-2-yl)-1H-indole-3-carbaldehyde (**15**). Following general method I, the compound **15** was obtained from **o** and 4-(dimethylamino)butan-1-ol as a yellow solid (52 mg, 68%): m.p. 181.6-183.1 °C; ^1H NMR (400 MHz, $\text{DMSO}-d_6$) δ 12.64 (s, 1H), 11.29 (s, 1H), 8.31 (d, $J = 7.9$ Hz, 1H), 8.26 (d, $J = 8.0$ Hz, 1H), 8.09 – 8.01 (m, 2H), 7.75 (t, $J = 7.8$ Hz, 1H), 7.70 (d, $J = 8.1$ Hz, 1H), 7.36 (t, $J = 7.5$ Hz, 1H), 7.28 (t, $J = 7.5$ Hz, 1H), 4.79 (t, $J = 5.0$ Hz, 2H), 3.19 (t, $J = 7.5$ Hz, 2H), 2.73 (s, 6H), 2.04 – 1.88 (m, 4H). ^{13}C NMR (101 MHz, $\text{DMSO}-d_6$) δ 189.8, 166.8, 154.0, 151.1, 142.0, 136.4, 135.4, 128.6, 128.1, 126.6, 125.3, 124.2, 123.4, 122.6, 117.3, 115.4, 113.4, 67.4, 45.8, 42.5 (2C), 25.8, 21.2. Purity: 97.5% by HPLC. HRMS (ESI) m/z :

calcd for $C_{23}H_{24}N_4O_2$, $[M+H]^+$ 389.1972, found 389.1977.

2-(4-(2-(Pyrrolidin-1-yl)ethoxy)quinazolin-2-yl)-1H-indole-3-carbaldehyde (**16**). Following general method I, the compound **16** was obtained from **o** and 2-(pyrrolidin-1-yl)ethan-1-ol as a pale yellow solid (64 mg, 85%): m.p. 213.3-215.1 °C; 1H NMR (400 MHz, $CDCl_3$) δ 11.46 (s, 1H), 10.45 (s, 1H), 8.53 (d, $J = 7.7$ Hz, 1H), 8.20 (d, $J = 8.1$ Hz, 1H), 7.98 (d, $J = 8.4$ Hz, 1H), 7.89 (t, $J = 7.6$ Hz, 1H), 7.60 (t, $J = 7.6$ Hz, 2H), 7.38 (t, $J = 7.5$ Hz, 1H), 7.35 – 7.30 (m, 1H), 4.98 (br, 2H), 3.25 – 3.19 (m, 2H), 2.90 (br, 4H), 1.93 (br, 4H). ^{13}C NMR (101 MHz, $DMSO-d_6$) δ 189.8, 166.5, 153.9, 151.2, 141.9, 136.4, 135.5, 128.7, 128.1, 126.6, 125.3, 124.5, 123.4, 122.6, 117.4, 115.3, 113.4, 54.3 (2C), 53.3, 23.4 (2C). Purity: 99.9% by HPLC. HRMS (ESI) m/z : calcd for $C_{23}H_{22}N_4O_2$, $[M+H]^+$ 387.1816, found 387.1811.

2-(4-(3-(Pyrrolidin-1-yl)propoxy)quinazolin-2-yl)-1H-indole-3-carbaldehyde (**17**). Following general method I, the compound **17** was obtained from **o** and 3-(pyrrolidin-1-yl)propan-1-ol as a pale yellow solid (60 mg, 78%): m.p. 73.8-76.0 °C; 1H NMR (400 MHz, $DMSO-d_6$) δ 12.58 (s, 1H), 11.29 (s, 1H), 8.31 (d, $J = 7.9$ Hz, 1H), 8.23 (d, $J = 8.0$ Hz, 1H), 8.09 – 8.00 (m, 2H), 7.75 (t, $J = 7.2$ Hz, 1H), 7.68 (d, $J = 8.1$ Hz, 1H), 7.36 (t, $J = 7.6$ Hz, 1H), 7.27 (t, $J = 7.5$ Hz, 1H), 4.80 (t, $J = 6.2$ Hz, 2H), 2.74 (br, 2H), 2.56 (br, 4H), 2.17 – 2.07 (m, 2H), 1.70 (br, 4H). ^{13}C NMR (101 MHz, $DMSO-d_6$) δ 189.7, 166.9, 154.1, 151.1, 142.1, 136.4, 135.3, 128.6, 128.1, 126.6, 125.3, 124.1, 123.3, 122.6, 117.4, 115.4, 113.3, 66.5, 54.1(2C), 49.1, 27.9, 23.5 (2C). Purity: 99.5% by HPLC. HRMS (ESI) m/z : calcd for $C_{24}H_{24}N_4O_2$, $[M+H]^+$ 401.1972, found 401.1964.

2-(4-((2-(Dimethylamino)ethyl)amino)quinazolin-2-yl)-5-methoxy-1H-indole-3-carbaldehyde (**18**). Following general method J, the compound **18** was obtained from **p** and *N,N*-dimethylethane-1,2-diamine as a brown solid (44 mg, 26%): m.p. 185.5-190.4 °C; 1H NMR (400

MHz, DMSO- d_6) δ 12.28 (s, 1H), 11.30 (s, 1H), 8.48 (br, 1H), 8.29 (d, $J = 3.7$ Hz, 1H), 7.89 – 7.77 (m, 3H), 7.56 (br, 2H), 6.95 (d, $J = 5.8$ Hz, 1H), 3.81 (br, 5H), 2.61 (br, 2H), 2.25 (s, 6H). ^{13}C NMR (101 MHz, DMSO- d_6) δ 190.0, 160.0, 156.5, 154.8, 149.6, 143.6, 133.7, 131.0, 128.2, 127.4, 126.6, 123.4, 116.7, 115.3, 114.5, 114.2, 103.3, 58.0, 55.7, 45.8 (2C), 39.4. Purity: 99.9% by HPLC. HRMS (ESI) m/z : calcd for $\text{C}_{22}\text{H}_{23}\text{N}_5\text{O}_2$, $[\text{M}+\text{H}]^+$ 390.1925, found 390.1929.

2-(4-((3-(Dimethylamino)propyl)amino)quinazolin-2-yl)-5-methoxy-1H-indole-3-carbaldehyde (19).

Following general method J, the compound **19** was obtained from **p** and *N,N*-dimethylpropane-1,3-diamine as a red-orange solid (132 mg, 74%): m.p.234.5-235.0 °C. ^1H NMR (400 MHz, DMSO- d_6) δ 12.44 (s, 1H), 11.30 (s, 1H), 9.02 (t, $J = 5.4$ Hz, 1H), 8.51 (d, $J = 8.3$ Hz, 1H), 7.86 – 7.81 (m, 2H), 7.80 (d, $J = 2.4$ Hz, 1H), 7.70 (d, $J = 8.9$ Hz, 1H), 7.59 – 7.54 (m, 1H), 6.97 (dd, $J = 8.9, 2.5$ Hz, 1H), 3.90 – 3.85 (m, 2H), 3.83 (s, 3H), 3.08 (t, $J = 7.0$ Hz, 2H), 2.64 (s, 6H), 2.16 – 2.06 (m, 2H). ^{13}C NMR (101 MHz, DMSO- d_6) δ 190.2, 160.1, 156.5, 154.8, 149.7, 143.6, 133.7, 131.0, 128.2, 127.4, 126.6, 123.9, 116.6, 115.2, 114.6, 114.4, 103.2, 55.7, 55.5, 43.1 (2C), 38.7, 24.6. Purity: 99.7% by HPLC. HRMS (ESI) m/z : calcd for $\text{C}_{23}\text{H}_{25}\text{N}_5\text{O}_2$, $[\text{M}+\text{H}]^+$ 404.2081, found 404.2085.

2-(4-((4-(Diethylamino)butyl)amino)quinazolin-2-yl)-5-methoxy-1H-indole-3-carbaldehyde (20).

Following general method J, the compound **20** was obtained from **p** and *N,N*-diethylbutane-1,4-diamine as a red-orange solid (116 mg, 63%): m.p.84.5-84.9 °C; ^1H NMR (400 MHz, DMSO- d_6) δ 12.26 (s, 1H), 11.29 (s, 1H), 8.73 (t, $J = 5.2$ Hz, 1H), 8.41 (d, $J = 8.3$ Hz, 1H), 7.89 – 7.82 (m, 2H), 7.79 (d, $J = 2.3$ Hz, 1H), 7.63 – 7.53 (m, 2H), 6.96 (dd, $J = 8.9, 2.4$ Hz, 1H), 3.82 (s, 3H), 3.76 (d, $J = 5.0$ Hz, 2H), 3.07 (br, 6H), 1.80 (br, 4H), 1.17 (t, $J = 7.2$ Hz, 6H). ^{13}C NMR (101 MHz, DMSO- d_6) δ 190.1, 160.1, 156.5, 154.9, 149.7, 143.7, 133.7, 131.1, 128.2, 127.4,

126.6, 123.7, 116.7, 115.3, 114.6, 114.2, 103.3, 55.7, 51.0, 46.5 (2C), 40.5, 26.1, 21.3, 8.9 (2C).

Purity: 100% by HPLC. HRMS (ESI) m/z : calcd for $C_{26}H_{31}N_5O_2$, $[M+H]^+$ 446.2551, found 446.2558.

5-Methoxy-2-(4-((2-(pyrrolidin-1-yl)ethyl)amino)quinazolin-2-yl)-1H-indole-3-carbaldehyde (21).

Following general method J, the compound **21** was obtained from **p** and 2-(pyrrolidin-1-yl)ethanamine as a pale yellow solid (110 mg, 60%): m.p.153.2-154.8 °C; 1H NMR (400 MHz, $CDCl_3$) δ 11.33 (s, 1H), 10.33 (s, 1H), 8.11 (d, $J = 7.9$ Hz, 1H), 7.92 (s, 1H), 7.84 (s, 1H), 7.73 (d, $J = 8.1$ Hz, 1H), 7.66 (t, $J = 7.5$ Hz, 1H), 7.43 (t, $J = 7.4$ Hz, 1H), 7.35 (d, $J = 8.5$ Hz, 1H), 6.91 (dd, $J = 8.7, 2.1$ Hz, 1H), 3.93 – 3.88 (m, 2H), 3.85 (s, 3H), 3.11 (t, $J = 4.1$ Hz, 2H), 2.98 (br, 4H), 1.98 – 1.90 (m, 4H). ^{13}C NMR (101 MHz, $CDCl_3$) δ 189.6, 158.7, 155.8, 152.9, 148.5, 141.8, 132.3, 129.0, 127.1, 126.8, 125.8, 121.5, 116.3, 115.0, 113.4, 111.6, 102.8, 54.8, 53.7, 53.1 (2C), 37.5, 22.4 (2C). Purity: 99.6% by HPLC. HRMS (ESI) m/z : calcd for $C_{24}H_{25}N_5O_2$, $[M+H]^+$ 416.2081, found 416.2090.

5-Methoxy-2-(4-((3-(pyrrolidin-1-yl)propyl)amino)quinazolin-2-yl)-1H-indole-3-carbaldehyde

(22). Following general method J, the compound **22** was obtained from **p** and 3-(pyrrolidin-1-yl)propan-1-amine as a yellow solid (74 mg, 39%): m.p.124.4-125.3 °C; 1H NMR (400 MHz, $DMSO-d_6$) δ 12.29 (s, 1H), 11.33 (s, 1H), 8.79 (s, 1H), 8.31 (d, $J = 7.8$ Hz, 1H), 7.89 – 7.77 (m, 3H), 7.65 – 7.53 (m, 2H), 6.99 (d, $J = 8.3$ Hz, 1H), 3.85 (s, 3H), 3.78 (t, $J = 3.8$ Hz, 2H), 2.66 (br, 2H), 2.56 (br, 4H), 1.97 – 1.88 (m, 2H), 1.72 (br, 4H). ^{13}C NMR (101 MHz, $MeOD-d_4$) δ 191.2, 159.8, 156.8, 154.3, 149.4, 144.1, 132.6, 130.6, 127.7, 127.2, 126.0, 121.8, 116.5, 114.9, 114.1, 112.7, 103.1, 54.6, 53.7 (2C), 53.6, 39.2, 26.9, 22.7 (2C). Purity: 99.9% by HPLC. HRMS (ESI) m/z : calcd for $C_{25}H_{27}N_5O_2$, $[M+H]^+$ 430.2238, found 430.2245.

5-Methoxy-2-(4-((4-(pyrrolidin-1-yl)butyl)amino)quinazolin-2-yl)-1H-indole-3-carbaldehyde (23).

Following general method J, the compound **23** (also named as **IQZ23**) was obtained from **p** and 4-(pyrrolidin-1-yl)butan-1-amine as a red-orange solid (95 mg, 49%): m.p.95.1-96.4 °C; ¹H NMR (400 MHz, DMSO-*d*₆) δ 12.20 (s, 1H), 11.30 (s, 1H), 8.54 (t, *J* = 5.3 Hz, 1H), 8.31 (d, *J* = 8.2 Hz, 1H), 7.83 – 7.81 (m, 2H), 7.79 (d, *J* = 2.4 Hz, 1H), 7.59 – 7.53 (m, 2H), 6.96 (dd, *J* = 8.8, 2.5 Hz, 1H), 3.82 (s, 3H), 3.70 (q, *J* = 6.7 Hz, 2H), 2.46 (d, *J* = 7.9 Hz, 2H), 2.43 (br, 4H), 1.80 – 1.72 (m, 2H), 1.67 – 1.61 (m, 4H), 1.61 – 1.54 (m, 2H). ¹³C NMR (101 MHz, DMSO-*d*₆) δ 190.1, 160.0, 156.5, 154.9, 149.7, 143.6, 133.6, 131.0, 128.1, 127.4, 126.6, 123.4, 116.8, 115.3, 114.6, 114.1, 103.3, 55.7, 55.7, 54.0 (2C), 41.3, 27.0, 26.3, 23.5 (2C). Purity: 98.6% by HPLC. HRMS (ESI) *m/z*: calcd for C₂₆H₂₉N₅O₂, [M+H]⁺ 444.2394, found 444.2381.

N¹,N¹-Dimethyl-N²-(2-(3-methyl-1H-indol-2-yl)quinazolin-4-yl)ethane-1,2-diamine (24).

Following general method K, the compound **24** was obtained from **u** and *N,N*-dimethylethane-1,2-diamine as a white solid (110 mg, 94%): m.p.131.0-132.4 °C; ¹H NMR (400 MHz, DMSO-*d*₆) δ 11.14 (s, 1H), 8.22 (d, *J* = 8.0 Hz, 2H), 7.80 – 7.70 (m, 2H), 7.60 (d, *J* = 7.9 Hz, 1H), 7.51 (d, *J* = 8.1 Hz, 1H), 7.48 – 7.42 (m, 1H), 7.16 (t, *J* = 7.5 Hz, 1H), 7.01 (t, *J* = 7.4 Hz, 1H), 3.83 (q, *J* = 6.3 Hz, 2H), 2.83 (s, 3H), 2.63 (t, *J* = 6.7 Hz, 2H), 2.25 (s, 6H). ¹³C NMR (101 MHz, DMSO-*d*₆) δ 159.8, 157.2, 150.2, 136.3, 133.2, 132.5, 129.9, 127.7, 125.3, 123.4, 123.2, 119.7, 119.0, 113.9, 113.7, 112.4, 58.2, 45.8 (2C), 39.4, 11.2. Purity: 99.7% by HPLC. HRMS (ESI) *m/z*: calcd for C₂₁H₂₃N₅, [M+H]⁺ 346.2026, found 346.2016.

N¹,N¹-Dimethyl-N³-(2-(3-methyl-1H-indol-2-yl)quinazolin-4-yl)propane-1,3-diamine (25).

Following general method K, the compound **25** was obtained from **u** and *N,N*-dimethylpropane-1,3-diamine as a pale yellow solid (113 mg, 93%): m.p.109.3-110.7 °C; ¹H

NMR (400 MHz, DMSO- d_6) δ 11.09 (s, 1H), 8.39 (t, J = 5.0 Hz, 1H), 8.20 (d, J = 8.3 Hz, 1H), 7.80 – 7.72 (m, 2H), 7.60 (d, J = 7.9 Hz, 1H), 7.51 (d, J = 8.1 Hz, 1H), 7.49 – 7.42 (m, 1H), 7.16 (t, J = 8.0, 7.1 Hz, 1H), 7.01 (t, J = 7.4 Hz, 1H), 3.75 (q, J = 6.7 Hz, 2H), 2.83 (s, 3H), 2.40 (t, J = 7.1 Hz, 2H), 2.20 (s, 6H), 1.93 – 1.84 (m, 2H). ^{13}C NMR (101 MHz, DMSO- d_6) δ 159.8, 157.3, 150.3, 136.3, 133.1, 132.5, 129.8, 127.7, 125.3, 123.4, 123.2, 119.7, 119.0, 113.9, 113.7, 112.4, 57.6, 45.6 (2C), 39.4, 27.0, 11.2. Purity: 99.3% by HPLC. HRMS (ESI) m/z : calcd for $\text{C}_{22}\text{H}_{25}\text{N}_5$, $[\text{M}+\text{H}]^+$ 360.2183, found 360.2176.

N¹,N¹-Dimethyl-N⁴-(2-(3-methyl-1H-indol-2-yl)quinazolin-4-yl)butane-1,4-diamine (26).

Following general method K, the compound **26** was obtained from **u** and *N,N*-dimethylbutane-1,4-diamine as a brown product (102 mg, 80%): m.p.97.3-98.5 °C; ^1H NMR (400 MHz, DMSO- d_6) δ 11.08 (s, 1H), 8.36 – 8.29 (m, 1H), 8.24 (d, J = 8.3 Hz, 1H), 7.80 – 7.72 (m, 2H), 7.60 (d, J = 7.7 Hz, 1H), 7.50 (d, J = 8.1 Hz, 1H), 7.48 – 7.38 (m, 1H), 7.16 (t, J = 7.4 Hz, 1H), 7.01 (t, J = 7.4 Hz, 1H), 3.73 (q, J = 6.5 Hz, 2H), 2.82 (s, 3H), 2.40 – 2.33 (m, 2H), 2.19 (s, 6H), 1.80 – 1.72 (m, 2H), 1.62 – 1.55 (m, 2H). ^{13}C NMR (101 MHz, DMSO- d_6) δ 159.8, 157.2, 150.2, 136.3, 133.2, 132.5, 129.9, 127.7, 125.2, 123.4, 123.2, 119.7, 119.0, 113.9, 113.7, 112.4, 59.1, 45.3 (2C), 41.1, 26.9, 24.9, 11.2. Purity: 99.4% by HPLC. HRMS (ESI) m/z : calcd for $\text{C}_{23}\text{H}_{27}\text{N}_5$, $[\text{M}+\text{H}]^+$ 374.2339, found 374.2328.

2-(3-Methyl-1H-indol-2-yl)-N-(2-(pyrrolidin-1-yl)ethyl)quinazolin-4-amine (27). Following

general method K, the compound **27** was obtained from **u** and 2-(pyrrolidin-1-yl)ethanamine as a pale yellow solid (123 mg, 98%): m.p.90.0-91.4 °C; ^1H NMR (400 MHz, DMSO- d_6) δ 11.10 (s, 1H), 8.29 – 8.21 (m, 2H), 7.80 – 7.72 (m, 2H), 7.60 (d, J = 8.0 Hz, 1H), 7.50 (d, J = 8.1 Hz, 1H), 7.46 (t, J = 7.1 Hz, 1H), 7.16 (t, J = 7.5 Hz, 1H), 7.01 (t, J = 7.4 Hz, 1H), 3.86 (q, J = 6.5 Hz, 2H), 2.85 – 2.77

(m, 5H), 2.57 (br, 4H), 1.70 (br, 4H). ^{13}C NMR (101 MHz, DMSO- d_6) δ 159.8, 157.2, 150.2, 136.3, 133.2, 132.5, 129.9, 127.7, 125.2, 123.4, 123.3, 119.7, 119.0, 113.9, 113.7, 112.4, 54.9, 54.3 (2C), 49.1, 23.7 (2C), 11.3. Purity: 95.3% by HPLC. HRMS (ESI) m/z : calcd for $\text{C}_{23}\text{H}_{25}\text{N}_5$, $[\text{M}+\text{H}]^+$ 372.2183, found 372.2167.

2-(3-Methyl-1H-indol-2-yl)-N-(3-(pyrrolidin-1-yl)propyl)quinazolin-4-amine (28). Following general method K, the compound **28** was obtained from **u** and 3-(pyrrolidin-1-yl)propan-1-amine as a yellow solid (113 mg, 86%): m.p.108.0-109.2 °C; ^1H NMR (400 MHz, CDCl_3) δ 9.92 (s, 1H), 8.55 (s, 1H), 7.66 (d, $J = 8.3$ Hz, 1H), 7.53 (d, $J = 7.9$ Hz, 1H), 7.50 – 7.42 (m, 2H), 7.17 – 7.09 (m, 2H), 7.05 (t, $J = 7.3$ Hz, 1H), 6.96 (t, $J = 7.4$ Hz, 1H), 3.65 (q, $J = 5.3$ Hz, 2H), 2.78 (s, 3H), 2.60 – 2.52 (m, 2H), 2.45 (br, 4H), 1.72 (br, 6H). ^{13}C NMR (101 MHz, CDCl_3) δ 158.5, 156.2, 148.9, 134.6, 131.2, 131.1, 129.2, 126.7, 123.5, 122.3, 120.3, 118.7, 117.8, 113.9, 112.8, 110.1, 54.8, 53.0 (2C), 41.3, 24.5, 22.4 (2C), 9.9. Purity: 99.8% by HPLC. HRMS (ESI) m/z : calcd for $\text{C}_{24}\text{H}_{27}\text{N}_5$, $[\text{M}+\text{H}]^+$ 386.2339, found 386.2343.

N^1,N^1 -Diethyl- N^2 -(2-(3-methyl-1H-indol-2-yl)quinazolin-4-yl)ethane-1,2-diamine (29). Following general method K, the compound **29** was obtained from **u** and *N,N*-diethylethane-1,2-diamine as a pale yellow solid (102 mg, 81%): m.p.101.5-101.9 °C; ^1H NMR (400 MHz, DMSO- d_6) δ 11.08 (s, 1H), 8.25 – 8.13 (m, 2H), 7.81 – 7.72 (m, 2H), 7.60 (d, $J = 7.7$ Hz, 1H), 7.55 – 7.41 (m, 2H), 7.15 (t, $J = 7.5$ Hz, 1H), 7.01 (t, $J = 7.3$ Hz, 1H), 3.81 (q, $J = 5.8$ Hz, 2H), 2.83 (s, 3H), 2.76 (t, $J = 7.1$ Hz, 2H), 2.58 (q, $J = 6.8$ Hz, 4H), 0.98 (t, $J = 7.1$ Hz, 6H). ^{13}C NMR (101 MHz, DMSO- d_6) δ 159.8, 157.2, 150.2, 136.3, 133.1, 132.5, 129.9, 127.7, 125.2, 123.4, 123.1, 119.7, 119.0, 113.9, 113.6, 112.3, 51.8, 47.3 (2C), 39.7, 12.4 (2C), 11.2. Purity: 99.9% by HPLC. HRMS (ESI) m/z : calcd for $\text{C}_{23}\text{H}_{27}\text{N}_5$, $[\text{M}+\text{H}]^+$ 374.2339, found 374.2326.

N¹,N¹-Diethyl-N⁴-(2-(3-methyl-1H-indol-2-yl)quinazolin-4-yl)butane-1,4-diamine (30). Following general method K, the compound **30** was obtained from **u** and *N,N*-diethylbutane-1,4-diamine as a yellow solid (78 mg, 57%): m.p. 138.2-138.9 °C; ¹H NMR (400 MHz, DMSO-*d*₆) δ 11.11 (s, 1H), 8.36 (s, 1H), 8.26 (d, *J* = 8.1 Hz, 1H), 7.79 – 7.71 (m, 2H), 7.59 (d, *J* = 7.9 Hz, 1H), 7.50 (d, *J* = 8.1 Hz, 1H), 7.45 (t, *J* = 7.0 Hz, 1H), 7.16 (t, *J* = 7.4 Hz, 1H), 7.01 (t, *J* = 7.3 Hz, 1H), 3.74 (q, *J* = 5.7 Hz, 2H), 2.82 (s, 3H), 2.65 (br, 6H), 1.81 – 1.71 (m, 2H), 1.67 – 1.57 (m, 2H), 1.00 (t, *J* = 6.3 Hz, 6H). ¹³C NMR (101 MHz, DMSO-*d*₆) δ 159.8, 157.2, 150.3, 136.3, 133.1, 132.5, 129.9, 127.7, 125.1, 123.3, 123.3, 119.6, 119.0, 113.9, 113.6, 112.4, 52.1, 46.7 (2C), 41.0, 26.9, 23.7, 11.1, 11.0 (2C). Purity: 99.9% by HPLC. HRMS (ESI) *m/z*: calcd for C₂₅H₃₁N₅, [M+H]⁺ 402.2652, found 402.2646.

N,N-Dimethyl-2-((2-(3-methylbenzofuran-2-yl)quinazolin-4-yl)oxy)ethan-1-amine (**31**). Following general method I, the compound **31** was obtained from **t** and 2-(dimethylamino)ethan-1-ol as a white solid (60 mg, 86%): m.p. 81.8-83.8 °C; ¹H NMR (400 MHz, CDCl₃) δ 8.20 (d, *J* = 8.0 Hz, 1H), 8.13 (d, *J* = 8.3 Hz, 1H), 7.86 (t, *J* = 7.6 Hz, 1H), 7.68 (t, *J* = 6.7 Hz, 2H), 7.55 (t, *J* = 7.4 Hz, 1H), 7.42 (t, *J* = 7.6 Hz, 1H), 7.32 (d, *J* = 7.3 Hz, 1H), 4.84 (t, *J* = 5.5 Hz, 2H), 2.96 (t, *J* = 5.4 Hz, 2H), 2.88 (s, 3H), 2.45 (s, 6H). ¹³C NMR (101 MHz, CDCl₃) δ 166.4, 154.8, 154.6, 151.6, 148.1, 133.8, 130.7, 128.1, 126.7, 126.3, 123.6, 122.7, 120.9, 120.3, 115.1, 112.1, 65.6, 57.9, 46.0 (2C), 10.4. Purity: 99.5% by HPLC. HRMS (ESI) *m/z*: calcd for C₂₁H₂₁N₃O₂, [M+H]⁺ 348.1707, found 348.1703.

N,N-Dimethyl-3-((2-(3-methylbenzofuran-2-yl)quinazolin-4-yl)oxy)propan-1-amine (**32**).

Following general method I, the compound **32** was obtained from **t** and 3-(dimethylamino)propan-1-ol as a white solid (51 mg, 70%): m.p. 198.6-200.1 °C; ¹H NMR (400 MHz, CDCl₃) δ 8.13 (t, *J* = 8.0 Hz, 2H), 7.86 (t, *J* = 7.7 Hz, 1H), 7.66 (d, *J* = 8.5 Hz, 2H), 7.55 (t, *J* = 8.0 Hz, 1H), 7.40 (t, *J* = 8.1 Hz, 1H), 7.31 (t, *J* = 7.7 Hz, 1H), 4.80 (t, *J* = 6.0 Hz, 2H), 3.03 (br,

2H), 2.85 (s, 3H), 2.68 (s, 6H), 2.50 – 2.38 (m, 2H). ^{13}C NMR (101 MHz, CDCl_3) δ 166.1, 154.7, 154.5, 151.6, 147.9, 134.0, 130.6, 128.2, 126.9, 126.4, 123.3, 122.8, 121.1, 120.4, 114.8, 112.1, 64.9, 55.7, 43.8 (2C), 25.7, 10.5. Purity: 99.9% by HPLC. HRMS (ESI) m/z : calcd for $\text{C}_{22}\text{H}_{23}\text{N}_3\text{O}_2$, $[\text{M}+\text{H}]^+$ 362.1863, found 362.1855.

N,N-Dimethyl-4-((2-(3-methylbenzofuran-2-yl)quinazolin-4-yl)oxy)butan-1-amine (**33**). Following general method I, the compound **33** was obtained from **t** and 4-(dimethylamino)butan-1-ol as a white solid (52 mg, 70%): m.p. 47.4-49.8 °C; ^1H NMR (400 MHz, CDCl_3) δ 8.16 (d, $J = 8.0$ Hz, 1H), 8.11 (d, $J = 8.4$ Hz, 1H), 7.84 (t, $J = 7.6$ Hz, 1H), 7.71 – 7.62 (m, 2H), 7.53 (t, $J = 7.5$ Hz, 1H), 7.40 (t, $J = 7.5$ Hz, 1H), 7.30 (d, $J = 8.0$ Hz, 1H), 4.72 (t, $J = 6.2$ Hz, 2H), 2.86 (s, 3H), 2.58 – 2.44 (m, 2H), 2.32 (s, 6H), 2.05 – 1.98 (m, 2H), 1.85 – 1.76 (m, 2H). ^{13}C NMR (101 MHz, CDCl_3) δ 166.5, 154.9, 154.5, 151.5, 148.1, 133.8, 130.7, 128.1, 126.7, 126.3, 123.5, 122.7, 120.9, 120.3, 115.1, 112.1, 67.2, 59.3, 45.3 (2C), 26.7, 24.1, 10.4. Purity: 99.7% by HPLC. HRMS (ESI) m/z : calcd for $\text{C}_{23}\text{H}_{25}\text{N}_3\text{O}_2$, $[\text{M}+\text{H}]^+$ 376.2020, found 376.2026.

2-(3-Methylbenzofuran-2-yl)-4-(2-(pyrrolidin-1-yl)ethoxy)quinazoline (**34**). Following general method I, the compound **34** was obtained from **t** and 2-(pyrrolidin-1-yl)ethan-1-ol as a white solid (67 mg, 90%): m.p. 69.6-71.7 °C; ^1H NMR (400 MHz, CDCl_3) δ 8.17 (d, $J = 8.1$ Hz, 1H), 8.11 (d, $J = 8.4$ Hz, 1H), 7.83 (t, $J = 7.7$ Hz, 1H), 7.65 (t, $J = 7.2$ Hz, 2H), 7.53 (t, $J = 7.6$ Hz, 1H), 7.39 (t, $J = 7.6$ Hz, 1H), 7.30 (d, $J = 7.5$ Hz, 1H), 4.85 (t, $J = 5.7$ Hz, 2H), 3.10 (t, $J = 5.7$ Hz, 2H), 2.85 (s, 3H), 2.74 (br, 4H), 1.85 (br 4H). ^{13}C NMR (101 MHz, CDCl_3) δ 166.3, 154.8, 154.6, 151.6, 148.0, 133.8, 130.7, 128.1, 126.7, 126.3, 123.6, 122.7, 120.9, 120.3, 115.1, 112.1, 66.7, 54.9 (2C), 54.5, 23.6 (2C), 10.4. Purity: 99.9% by HPLC. HRMS (ESI) m/z : calcd for $\text{C}_{23}\text{H}_{23}\text{N}_3\text{O}_2$, $[\text{M}+\text{H}]^+$ 374.1863, found 374.1870.

2-(3-Methylbenzofuran-2-yl)-4-(3-(pyrrolidin-1-yl)propoxy)quinazoline (35). Following general method I, the compound **35** was obtained from **t** and 3-(pyrrolidin-1-yl)propan-1-ol as a white solid (61 mg, 78%): m.p. 186.6-187.5 °C; ¹H NMR (400 MHz, CDCl₃) δ 8.13 (t, *J* = 8.5 Hz, 2H), 7.86 (t, *J* = 7.7 Hz, 1H), 7.67 (d, *J* = 8.6 Hz, 2H), 7.55 (t, *J* = 7.5 Hz, 1H), 7.41 (t, *J* = 8.1 Hz, 1H), 7.31 (t, *J* = 7.7 Hz, 1H), 4.79 (t, *J* = 5.9 Hz, 2H), 3.21 – 2.90 (m, 6H), 2.85 (s, 3H), 2.52 – 2.40 (m, 2H), 2.03 (br, 4H). ¹³C NMR (101 MHz, CDCl₃) δ 166.1, 154.7, 154.5, 151.6, 147.8, 134.0, 130.6, 128.2, 126.9, 126.4, 123.3, 122.8, 121.1, 120.4, 114.8, 112.1, 65.0, 54.1 (2C), 53.3, 26.9, 23.5 (2C), 10.5. Purity: 99.9% by HPLC. HRMS (ESI) *m/z*: calcd for C₂₄H₂₅N₃O₂, [M+H]⁺ 388.2020, found 388.2015.

*N¹,N¹-Dimethyl-N²-(2-(3-methylbenzo[*b*]thiophen-2-yl)quinazolin-4-yl)ethane-1,2-diamine (36)*.

Following general method L, the compound **36** was obtained from **v** and *N,N*-dimethylethane-1,2-diamine as a white solid (67 mg, 58%): m.p. 125.7-127.7 °C; ¹H NMR (400 MHz, DMSO-*d*₆) δ 11.11 (s, 1H), 8.23 (d, *J* = 8.1 Hz, 1H), 7.79 – 7.71 (m, 2H), 7.59 (d, *J* = 7.9 Hz, 1H), 7.49 (d, *J* = 8.1 Hz, 1H), 7.45 (t, *J* = 6.3 Hz, 1H), 7.15 (t, *J* = 7.5 Hz, 1H), 7.01 (t, *J* = 7.4 Hz, 1H), 3.83 (q, *J* = 6.5 Hz, 2H), 2.82 (s, 3H), 2.62 (t, *J* = 6.8 Hz, 2H), 2.25 (s, 6H). ¹³C NMR (101 MHz, DMSO-*d*₆) δ 159.7, 158.7, 150.0, 142.1, 139.7, 138.8, 133.7, 133.2, 128.0, 126.0, 125.8, 124.4, 123.2, 123.2, 122.7, 113.9, 58.1, 45.8 (2C), 39.5, 14.0. Purity: 99.9% by HPLC. HRMS (ESI) *m/z*: calcd for C₂₁H₂₂N₄S, [M+H]⁺ 363.1638, found 363.1614.

*N¹,N¹-Dimethyl-N³-(2-(3-methylbenzo[*b*]thiophen-2-yl)quinazolin-4-yl)propane-1,3-diamine (37)*.

Following general method L, the compound **37** was obtained from **v** and *N,N*-dimethylpropane-1,3-diamine as a pale yellow solid (46 mg, 38%): m.p. 105.1-106.5 °C; ¹H NMR (400 MHz, DMSO-*d*₆) δ 8.49 (t, *J* = 5.3 Hz, 1H), 8.21 (d, *J* = 8.0 Hz, 1H), 7.97 – 7.91 (m, 1H), 7.91 – 7.85 (m, 1H), 7.78 (t, *J* = 7.5 Hz, 1H), 7.72 (d, *J* = 8.1 Hz, 1H), 7.49 (t, *J* = 8.1 Hz, 1H), 7.46

– 7.40 (m, 2H), 3.68 (q, $J = 6.7$ Hz, 2H), 3.02 (s, 3H), 2.40 (t, $J = 7.1$ Hz, 2H), 2.20 (s, 6H), 1.93 – 1.85 (m, 2H). ^{13}C NMR (101 MHz, DMSO- d_6) δ 159.7, 158.7, 145.0, 142.1, 139.6, 138.7, 133.7, 133.3, 128.0, 126.1, 125.9, 124.5, 123.3, 123.1, 122.7, 113.9, 57.6, 45.6 (2C), 40.0, 26.9, 14.0. Purity: 99.9% by HPLC. HRMS (ESI) m/z : calcd for $\text{C}_{22}\text{H}_{24}\text{N}_4\text{S}$, $[\text{M}+\text{H}]^+$ 377.1794, found 377.1785.

2-(3-Methylbenzo[b]thiophen-2-yl)-N-(2-(pyrrolidin-1-yl)ethyl)quinazolin-4-amine (38).

Following general method L, the compound **38** was obtained from **v** and 2-(pyrrolidin-1-yl)ethanamine as a yellow solid (110 mg, 89%): m.p. 88.2–91.0 °C; ^1H NMR (400 MHz, DMSO- d_6) δ 8.41 (t, $J = 4.4$ Hz, 1H), 8.24 (d, $J = 8.1$ Hz, 1H), 7.97 – 7.92 (m, 1H), 7.91 – 7.86 (m, 1H), 7.81 – 7.75 (m, 1H), 7.73 (d, $J = 7.5$ Hz, 1H), 7.50 (t, $J = 7.4$ Hz, 1H), 7.46 – 7.40 (m, 2H), 3.81 (q, $J = 6.3$ Hz, 2H), 3.02 (s, 3H), 2.84 (br, 2H), 2.61 (br, 4H), 1.72 (br, 4H). ^{13}C NMR (101 MHz, DMSO- d_6) δ 159.7, 158.6, 150.0, 142.1, 139.6, 138.6, 133.8, 133.4, 128.0, 126.1, 125.9, 124.6, 123.3, 123.3, 122.7, 113.8, 54.7, 54.2 (2C), 39.50, 23.6 (2C), 14.0. Purity: 98.5% by HPLC. HRMS (ESI) m/z : calcd for $\text{C}_{23}\text{H}_{24}\text{N}_4\text{S}$, $[\text{M}+\text{H}]^+$ 389.1794, found 389.1785.

2-(3-Methylbenzo[b]thiophen-2-yl)-N-(3-(pyrrolidin-1-yl)propyl)quinazolin-4-amine (39).

Following general method L, the compound **39** was obtained from **v** and 3-(pyrrolidin-1-yl)propan-1-amine as a white solid (111 mg, 86%): m.p. 127.5–129.0 °C; ^1H NMR (400 MHz, CDCl_3) δ 8.75 (s, 1H), 7.80 – 7.75 (m, 2H), 7.74 – 7.68 (m, 1H), 7.63 – 7.57 (m, 1H), 7.58 (d, $J = 8.2$ Hz, 1H), 7.34 – 7.23 (m, 3H), 3.79 (q, $J = 4.9$ Hz, 2H), 2.97 (s, 3H), 2.75 (t, $J = 6.8$ Hz, 2H), 2.61 (br, 4H), 1.96 – 1.88 (m, 2H), 1.86 – 1.84 (m, 4H). ^{13}C NMR (101 MHz, CDCl_3) δ 158.4, 158.3, 149.1, 141.2, 139.0, 137.6, 132.8, 131.2, 127.4, 124.1, 123.9, 122.6, 121.6, 121.2, 120.2, 112.8, 55.2, 53.2 (2C), 41.6, 24.6, 22.6 (2C), 12.8. Purity: 99.5% by HPLC. HRMS (ESI) m/z : calcd for $\text{C}_{24}\text{H}_{26}\text{N}_4\text{S}$, $[\text{M}+\text{H}]^+$ 403.1951, found 403.1950.

2-(3-Methylbenzo[b]thiophen-2-yl)-N-(4-(pyrrolidin-1-yl)butyl)quinazolin-4-amine (**40**).

Following general method L, the compound **40** was obtained from **v** and 4-(pyrrolidin-1-yl)butan-1-amine as a bright yellow product (88 mg, 66%): m.p. 80.0-81.6 °C; ¹H NMR (400 MHz, DMSO-*d*₆) δ 8.53 (t, *J* = 4.8 Hz, 1H), 8.29 (d, *J* = 8.2 Hz, 1H), 7.95 (t, *J* = 7.6 Hz, 1H), 7.87 (d, *J* = 8.0 Hz, 1H), 7.80 – 7.77 (m, 2H), 7.49 (t, *J* = 7.4 Hz, 1H), 7.46 – 7.39 (m, 2H), 3.67 (q, *J* = 6.0 Hz, 2H), 3.03 (s, 3H), 2.65 – 2.55 (m, 6H), 1.82 – 1.76 (m, 2H), 1.69 (br, 4H), 1.67 – 1.61 (m, 2H). ¹³C NMR (101 MHz, DMSO-*d*₆) δ 159.7, 158.7, 149.9, 142.1, 139.6, 138.7, 133.7, 133.3, 128.0, 126.1, 125.8, 124.5, 123.3, 123.3, 122.7, 113.9, 55.5, 53.8 (2C), 41.1, 26.8, 25.8, 23.4 (2C), 14.0. Purity: 98.9% by HPLC. HRMS (ESI) *m/z*: calcd for C₂₅H₂₈N₄S, [M+H]⁺ 417.2107, found 417.2089.

4.2. Pharmacology

4.2.1 Cell Lines and Cell culture.

3T3-L1 pre-adipocyte and C2C12 myoblast were obtained from American Type Culture Collection. The cells were maintained in DMEM (Geneon, USA) supplemented with 10% fetal bovine serum (BI, USA) and 1% penicillin and streptomycin (Gibco, USA) in a humidified atmosphere containing 5% CO₂ in air at 37 °C.

4.2.2 3T3-L1 Adipocyte Differentiation Assay.

Briefly, the 3T3-L1 fibroblast differentiation procedure was carried out as follows. After confluence (day 0), the cells were changed to a differentiation cocktail mixture containing 0.5 mM 3-isobutyl-1-methylxanthine (Sigma, USA), 100 ng/mL dexamethasone (MP, USA), and 2 µg/mL

insulin (Sigma, USA) in DMEM with 10% (v/v) FBS and 1% (v/v) penicillin and streptomycin for 3 days (day 3). Thereafter, the medium was replaced by 10% FBS/DMEM containing 2 $\mu\text{g}/\text{mL}$ insulin for another 3 days (day 6). Stock solutions of the test compounds were made and stored at $-20\text{ }^{\circ}\text{C}$. The compounds were added on day 0 in the differentiation induction medium for 3 days and replaced with another aliquot in post differentiation medium for another 3 days. The undifferentiation cells group (UND group) and the differentiation cell group (control group) were supplemented with the same volume of DMSO as vehicle control for all experiments.

4.2.3 Oil-red O Staining and TG Determination.

Oil Red O staining was performed as reported [26]. Briefly, the 0.3% ORO working solution was prepared by mixing 6 mL of 0.5% ORO (w/v in isopropanol, Sigma) with 4 mL of ddH₂O followed by filtration through a 0.22 μm filter (Millipore). The cells were washed with ice-cold PBS (pH7.4) and then fixed with 4% formaldehyde for 1 h at room temperature. The cells were stained with freshly prepared Oil Red O working solution for 30 min at room temperature in dark and washed twice with ddH₂O. The ORO staining images were captured using an OLYMPUS CKX41 microscope and camera (OLYMPUS, Japan). For TG determination, treated-cell were lysed with distilled water containing 0.2% Triton X-100 (MP Biomedicals, China) for 1 h at room temperature and then ultrasonicated for 15 min. The lysates were collected and centrifuged at $4\text{ }^{\circ}\text{C}$, 3 000g for 15 min. The triglyceride content of the cells was measured using GPO-POD assay kits (Jiancheng Bio, China), and the protein levels were determined using BCA protein assay kits (Pierce, USA). Then, the results were expressed as “mmol triglyceride / g protein” as previously described.²⁵ The TG level in control group cells was viewed as 100%, and the TG level in compounds treatment group was expressed as % of the control group.

4.2.4 Lactate Dehydrogenase (LDH) Releasing Assay.

The toxicity of compounds was determined by LDH releasing determined kit (Beyotime, China). After the cells were treated with the compounds for the 6 days, the plates were centrifuged at 3000 rpm for 5 min and supernatant was carefully collected and subjected to LDH activity determination according to the manufacturer's protocol. The absorbance of the samples was read at 490 nm with a microplate reader (Biotek, USA). The LDH releasing level was determined as followed: LDH releasing level (fold) = [(compound treated cell – blank group cell)/(control group cell – blank group cell)]. The LDH releasing level in control group was viewed as 1, then fold in compounds treatment group were calculated. Blank group: without treatment. Control group: without the compound treatment but added the same volume of DMSO as a compound treatment group. Compound treatment group: with the compound treatment. The higher level of the LDH releasing in compound treatment indicated more cytotoxicity of the treatment compounds in cells.

4.2.5 RNA Extraction and RT-qPCR.

Total RNA was extracted from cells using RNAiso Plus (Takara, China) according to the manufacturer's instructions. cDNA was synthesized by using Oligo dT from 1 µg of total RNA in a 20 µL reaction by reverse transcription kits (Takara, China), and cDNA was used for amplification of specific target gene by quantitative real-time PCR using the ABI Prism 7900 HT real-time PCR machine (Applied Biosystems) and the SYBR Green PCR Master Mix (Qiagen, China). β-actin was viewed as the internal control for normalization. The following SYBR Green primer sequences were synthesized by Generay Biotech (China) and listed in Table S2. The thermal cycle conditions were as follows: after heating at 95 °C for 10 min, PCR amplification was done with 30 cycles of

denaturation at 95 °C for 30 s, the respective annealing temperature (58~60 °C) for 45 s, extension at 72 °C for 1 min, followed by a terminal extension at 72 °C for 10 min.

4.2.6 Western Blot.

Cultured cells were washed with ice-cold PBS (pH 7.4), which were lysed with lysis buffer containing protease inhibitor cocktail (Roche, China) on ice for 0.5 h. Then, the lysates were centrifuged at 4 °C, 12000 g for 30 min to remove debris. The protein concentrations of the lysates were determined using a BCA protein assay kit (Thermo, China). Protein samples were denatured in 6-fold SDS loading buffer (Beyotime, China) and resolved by SDS-PAGE, then transferred to a polyvinylidene difluoride membrane (Millipore, China). After blocking with TBS/T (0.1%) containing 5% bovine serum albumin (BSA, Sigma) for 30 min at room temperature, the membrane was incubated with different primary antibodies at 4 °C overnight. The antibodies information used for Western blot were listed in Table S3. The membrane was washed with TBS/T for four times to remove the unbound antibody and then incubated with the HRP-conjugated secondary antibody (Cell Signaling Technology, China) for 1 h at room temperature. Representative images were captured, and densitometry analysis was performed using Quantity One Software (Bio-Rad Laboratories, USA) and relative protein levels were quantified by normalizing to loading control Actin.

4.2.7 Mouse Liver Microsome Stability and Aqueous Solubility Assay.

Aqueous solubility and mouse liver microsome stability measurements were performed as reported [27]. 5 μ L of 10 mM compound was added to 10 μ L of mouse liver microsomes (10 mg/mL) in 285 μ L of Tris-HCL (50 mM, pH7.4). Then 200 μ L of pre-warmed β -NADPH solution (3.3 mM MgCl_2 , 1.3 mM β -NADPN $_2$, 3.3 mM glucose-6-phosphate, 4 U/mL glucose-6-phosphate

dehydrogenase) was added to initiate the reaction at 37 °C. Aliquots of 40 µL of the mixture were collected at 0, 15, 30, 45, 60 min, and then proteins were precipitated with 500 µL of ice-cold acetonitrile. The supernatants were collected after centrifugation at 125000 g for 10 min and then the supernatant was subjected to LC–MS/MS analysis. The natural log of the amount of compound remaining was plotted against the time to determine the half-life of the tested compound. For aqueous solubility assay, eight 2-fold serial dilutions of the test compound with an initial concentration at 10 mM were prepared in DMSO. 1 µL of the compound solution is added to 199 µL of phosphate-buffered saline (pH 7.4) buffer, and the final compound concentrations range between 3.90 µM and 500 µM. After 24 h incubation, the solution was centrifuged, and the absorbance of supernatant is measured at the maximum absorbance of 340 nm and the kinetic solubility is estimated from the concentration of the test compound which has a higher absorbance than the background.

4.2.8 ATP Level Determination

ATP levels in 3T3-L1 adipocytes were quantified by using commercial ATP determination kit following the manufacturer's instructions (Promega, China) by normalized to protein level following the manufacturer's instructions.

4.2.9 siRNA Transfection

3T3-L1 cells (2×10^5) were seeded on a six-well plate (Corning, USA). After the density reached 80%, cells were transfected with 50 nM AMPK α siRNA or negative controls (RiboBio, China) for 24 h using Lipofectamine 3000 (Thermo, China) according to the manufacturer's instructions. After confluence, 3T3-L1 cells were exposed to adipogenic cocktail to induce adipocyte differentiation as

above described.

4.2.10 2-NBDG Assay

The glucose uptake assay was performed by using 2-NBDG probe as reported [28]. Briefly, after treatment, cells were washed with PBS and co-incubated with 30 μ M 2-NBDG (Thermo, China) and hocheist 33342 (for a nucleus, 1:1000) for 30 min in the dark at 37 °C. Microscopies were captured by Zeiss Confocal microscopy (Germany, Zeiss). The relative fluorescence of 2-NBDG was quantified by a fluorescence spectrophotometer using 488 nm Ex and 519 nm Em filter settings.

4.2.11 Mitochondria Copies Determination and Confocal Microscopy

Mitochondrial copies were measured by determining the ratio of mtDNA/nDNA [29]. Genome DNA from cells was extracted by using a DNA isolation kit (Sangon Biotech, China). The primers of cytochrome C (for mitochondrial) and 18S rRNA (for nucleus) used for PCR were listed in Table S2. The microscopy images were captured by using Mito-tracker probe (Thermo, China) [30]. Briefly, after treatment, cells were incubated with 1 μ M Mito-Tracker (for mitochondria) and hocheist 33342 probe (for a nucleus, 1:1000) (Thermo, China) in culture medium solution for 30 min in the dark at 37 °C. The microscopies were captured under the excitation of 633 nm and 405 nm.

4.2.12 Oxygen Consumption Ratio (OCR) determination

3T3-L1 cells were seeded in XF 96-well cell culture microplate in quintuplicate at 5000 cells/well in 0.1 mL growth medium and then incubated at 37 °C in 5% CO₂. Mitochondria isolated from tumors of mice were planted into XF 96-well cell culture and centrifuged at 2000 g for 5 min. Assays were initiated by removing the growth medium from each well and replacing it with 100 μ L of assay medium pre-warmed to 37 °C. The cells were incubated at 37 °C for 30 min to allow media

temperature and pH to reach equilibrium before the first-order rate measurement. Prior to each rate measurement, the XF-96 Analyser gently mixed the assay media in each well for 10 min to allow the oxygen partial pressure to reach equilibrium. Following mixing, OCR was measured simultaneously for 3–5 min to establish a baseline rate. The assay medium was then gently mixed again for 3–5 min between each rate measurement to restore normal oxygen tension and pH in the microenvironment surrounding the cells. After the baseline measurement, 5–20 μL of a testing agent prepared in assay medium was then injected into each well to reach the desired final working concentration. This was followed by mixing for 5–10 min to expedite compound exposure to cellular proteins, after which OCR measurements were then made. Generally, two to three baseline rates and two or more response rates (after compound addition) were measured, and the average of two baseline rates or test rates was used for data analysis. For time-resolved experiments, multiple measurements, as well as compound injections, were made at the time points indicated. The value of OCR reflects the metabolic activity of the cells and the number of cells being measured. Typically, at the end of each assay cells are treated for cell counted number.

4.2.13 Animal Study

Male C57BL/6J mice (aged 7–8 weeks) bred at the Laboratory Animal Centre of Sun Yat-sen University (Guangzhou, China) were used for the study. All animal procedures were approved by the Sun Yat-sen University Committee on Ethics for the Use of Laboratory Animals in accordance with the Animal Welfare Legislation of China. Animal studies are reported in compliance with the ARRIVE guidelines [31, 32]. The mice were kept at $22 \pm 1^\circ\text{C}$ on a 12 h light/dark cycle with free access to food and water. After 1 week of acclimatization to the environment of this study, mice were randomly assigned to receive either a chow diet (CH, with 70% calories from starch) or an HFC diet

(60% fat and 1% cholesterol, ResearchDiet, #12492) *ad libitum* for up to 14 weeks. HFC group mice were randomly divided into two subgroups at the beginning of week 9 to receive the treatment with **IQZ23** or its vehicle. **IQZ23** was dissolved in normal saline containing 10% ethanol and 10% castor oil and intraperitoneal injection at a dosage of 20 mg/kg every other day for 6 weeks. The control subgroup mice were administered the same volume of the vehicle. Bodyweight and food intake were monitored daily.

4.2.14 Acute Effect of 25 on Glucose Level

Mice were randomly divided into two subgroups: control group mice and **IQZ23**-treated mice. To determine the acute effect of **IQZ23** on glucose level, mice were intraperitoneal (*i.p.*) injection with saline (control group mice) or **IQZ23** (20 mg/kg) once time, the plasma glucose level was determined at 0, 0.5, 1, 2, 4, 8, 12, 24 h with a blood glucose monitor, respectively.

4.2.15 Glucose Tolerance Test (GTT) and Insulin Tolerance Test (ITT)

A glucose tolerance test (GTT) was performed as reported [33]. After 3 weeks of treatment with **IQZ23**, mice were fasted for a period of 6 h and then intraperitoneal injected with glucose (2 g/kg, Sigma, China). For ITT, after 6 weeks of treatment with **IQZ23**, mice have fasted for 6 h and intraperitoneally injected with 0.4 U insulin per mouse (Sigma, China). The glucose level was determined at 0, 15, 30, 60, 120 min after injection with a blood glucose monitor. Blood samples for both GTT and ITT were taken from the tail vein under local anesthesia with saline containing 2% lidocaine to ensure animal well-being and that it was not subjected to significant discomfort.

4.2.16 Chemical Determination in Plasma

At the end of the study, mice were fasted for 6 h and anesthetized by an *i.p.* injection of

ketamine/xylazine. After the mice were fully anesthetized, the eyeball was removed to collect blood samples in a tube containing 1mM EDTA (Hoff, 2000) for the measurement of relevant plasma parameters. After the blood samples were collected, the anesthetized mice were killed by cervical decapitation; the tissues of interest were weighed, freeze-clamped or fixed in a 4% formaldehyde solution. Plasma levels of TG, FFA, total cholesterol, LDL cholesterol, HDL cholesterol, alkaline phosphatase (ALP), alanine transaminase (ALT) and aspartate aminotransferase (AST), total protein, urea, blood urea nitrogen, creatinine, total bilirubin, and albumin were determined by an Olympus AU 600 auto-analyzer (Olympus, Japan). Plasma levels of insulin were detected using an ultra-sensitive insulin ELISA kit.

4.2.17 Histological Analysis

The tissues fixed in 4% formaldehyde solution were embedded in paraffin after dehydration in a graded ethanol series (70–100%). Embedded samples were sectioned (4 μm thick) with a rotary microtome and stained with hematoxylin and eosin (H&E), Oil-red O, and Sirius O for microscopic examination. Sections were viewed with a light microscope (Olympus) and photographed at $\times 200$ magnification. The section of the immunohistochemistry image was first labeled by an identification number code without the information of the grouping. The numbers and sizes of adipocytes of each slide were calculated with IMAGE J software (USA) by Servicebio Company (Beijing, China). Quantification analysis was performed in six randomly selected fields per sample in a blinded manner.

4.2.18 Pharmacokinetics Study

IQZ23 was dissolved in ethanol/saline (5: 95). Male Sprague-Dawley (SD) rats ($n = 3$) weighing

180-220 g were injected with these compounds intravenously (2 mg/kg) or intragastrically (5 mg/kg). Blood plasma samples were collected at 0, 30 min and 1h, 2 h, 4 h, 8 h, 12 h, 24 h after administration of compounds, and then immediately centrifuged (12000 rpm, 10 min) to obtain plasma samples. The concentration of compounds in plasma was measured by LC-MS/MS. The pharmacokinetic parameters were calculated using Kinetica 4.4 software.

4.2.19 Statistical analysis

Each experiment was repeated four times independently with three replicates. Results were expressed as mean \pm SEM and analyzed using GraphPad Prism 5 Software from three independent experiments. The Mann–Whitney and one-way ANOVA tests were used to compare data sets. Statistical significance was set at $p < 0.05$.

Conflict of interest

The authors declare no competing financial interest.

Acknowledgements

This work was supported by the National Natural Science Foundation of China (21672265, 81930098, and 81872732 to ZH, 81703336 to YR); the Special Fund for Science and Technology Development in Guangdong Province (2016A020217004 to ZH); the Science and Technology Program of Guangzhou (201704020104 to ZH), the Natural Science Foundation of Guangdong Province (2017A030308003 to ZH), the 111 Project (B16047), the Ministry of Education of China (IRT-17R111) and the Fundamental Research Funds for the Central Universities (31610915), the Local Innovative and Research Teams Project of Guangdong Pearl River Talents Program

(2017BT01Y093), the Guangdong Provincial Key Laboratory of Construction Foundation (2017B030314030).

Appendix A. Supporting information

Additional experimental results, ^1H and ^{13}C NMR spectra, HRMS and HPLC assay data for final compounds and a CSV file of molecular formula strings are available free of charge via the Internet at

References

- [1] Kopelman PG. Obesity as a medical problem. *Nature* 404 (2000) 635–643.
- [2] Ng M, Fleming T, Robinson, M, Thomson, B, Graetz, N, Margono, C, et al. Global, regional, and national prevalence of overweight and obesity in children and adults during 1980-2013: a systematic analysis for the global burden of disease study 2013. *Lancet* 2014; 384:766–781.
- [3] Masuzaki H, Paterson J, Shinyama H, Morton NM, Mullins JJ, Seckl JR, et al. A transgenic model of visceral obesity and the metabolic syndrome. *Science* 294 (2001) 2166–2170.
- [4] Rankin W, Wittert G. Anti-obesity drugs. *Curr. Opin. Lipidol.* 26 (2015) 536-543.
- [5] Bray GA, Fruhbeck, G, Ryan DH, Wilding J PH. Management of obesity. *Lancet* 387 (2016) 1947–1956.
- [6] Spiegelman BM, Flier JS. Obesity and the regulation of energy balance. *Cell* 104 (2001) 531–543.
- [7] Day EA, Ford RJ, Steinberg GR. AMPK as a therapeutic target for treating metabolic diseases. *Trends Endocrinol. Metab.* 28 (2017) 545–560.

- [8] Ruderman NB, Carling D, Prentki M, Cacicedo JM. AMPK, insulin resistance, and the metabolic syndrome. *J. Clin. Invest.* 123(2013) 2764–2772.
- [9] Garcia D, Shaw RJ. AMPK: Mechanisms of cellular energy sensing and restoration of metabolic balance. *Mol. Cell.* 66 (2017) 789–800.
- [10] Sharma H, Kumar S. Natural AMPK Activators: an alternative approach for the treatment and management of metabolic syndrome. *Curr. Med. Chem.* 24 (2017) 1007–1047.
- [11] Lee YS, Yang WK, Kim HY, Min B, Caturla N, Jones, J, et al. Metabolaid[®] combination of lemon verbena and hibiscus flower extract prevents high-fat diet-induced obesity through AMP-activated protein kinase activation. *Nutrients* 10 (2018) 1024–1041.
- [12] Park SH, Huh TL, Kim SY, Oh MR, Tirupathi Pichiah PB, Chae SW, et al. Antiobesity effect of *gynostemma pentaphyllum* extract (Actiponin): a randomized, double-blind, placebo-controlled trial. *Obesity* 23 (2015) 2520–2520.
- [13] Chang HP, Wang ML, Hsu CY, Liu ME, Chan MH, Chen YH. Suppression of inflammation-associated factors by indole-3-carbinol in mice fed high-fat diets and in isolated, co-cultured macrophages and adipocytes. *Int. J. Obes.* 35(2011) 1530–1538.
- [14] Van Huijsduijnen RH, Bombrun A, Swinnen D. Selecting protein tyrosine phosphatases as drug targets. *Drug. Discov. Today.* 7 (2002) 1013–1019.
- [15] Natural alkaloid bouchardatine ameliorates metabolic disorders in high-fat diet-fed mice by stimulating the sirtuin 1/liver kinase B-1/AMPK axis. *Br. J. Pharmacol.* 174 (2017) 2457–2470.
- [16] Rutaecarpine analogues reduce lipid accumulation in adipocytes via inhibiting adipogenesis/lipogenesis with AMPK activation and UPR suppression. *ACS. Chem. Biol.* 10

(2015) 1570-1571.

- [17] Synthesis and biological evaluation of novel bouchardatine derivatives as potential adipogenesis/lipogenesis inhibitors for anti-obesity treatment. *J. Med. Chem.* 58 (201) 9395–9413.
- [18] Gao L, Xu Z, Rao Y, Lu YT, Hu YT, Yu H, et al. Design, synthesis and biological evaluation of novel bouchardatine analogs as potential inhibitors of adipogenesis/lipogenesis in 3T3-L1 adipocytes. *Eur. J. Med. Chem.* 147 (2018) 90–101.
- [19] Censi R, Di Martino P. Polymorph impact on the bioavailability and stability of poorly soluble drugs. *Molecules* 20 (2015) 18759–18776.
- [20] Capsoni D, Quinzeni I, Bruni G, Friuli V, Maggi L, Bini M. Improving the carprofen solubility: synthesis of the Zn₂Al-LDH hybrid compound. *J. Pharm. Sci.* 107 (2018) 267–272.
- [21] Laplante M, Sabatini DM. An emerging role of mTOR in lipid biosynthesis. *Curr. Biol.* 19 (2019) R1046–1052.
- [22] Moseti D, Regassa A, Kim WK. Molecular regulation of adipogenesis and potential anti-adipogenic bioactive molecules. *Int. J. Mol. Sci.* 17 (2016) 124–147.
- [23] Kjøbsted R, Munk-Hansen N, Birk JB, Foretz M, Viollet B, Bjørnholm M, et al. Enhanced muscle insulin sensitivity after contraction/exercise is mediated by AMPK. *Diabetes* 66 (2017) 598–612.
- [24] Herzig S, Shaw RJ. AMPK: guardian of metabolism and mitochondrial homeostasis. *Nat. Rev. Mol. Cell. Biol.* 19 (2019) 121–135.
- [25] Choi W, Namkung J, Hwang I, Kim H, Lim A, Park HJ, et al. Serotonin signals through a gut-liver axis to regulate hepatic steatosis. *Nat. Commun.* 9 (2019) 4824–4832.

- [26] Maekawa T, Jin W, Ishii S. The role of ATF-2 family transcription factors in adipocyte differentiation: antiobesity effects of p38 inhibitors. *Mol. Cell. Biol.* 30 (2010) 613–625.
- [27] Shao H, Li XK, Moses MA, Gilbert LA, Kalyanaraman C, Young ZT, et al. Exploration of benzothiazole rhodacyanines as allosteric inhibitors of protein-protein interactions with heat shock protein 70 (Hsp70). *J. Med. Chem.* 61 (2018) 6163–6177.
- [28] Yamada K, Saito M, Matsuoka H, Inagaki N. A real-time method of imaging glucose uptake in single, living mammalian cells. *Nat. Protoc.* 2 (2007) 753–762.
- [29] Zhang Z, Zhang H, Li B, Meng X, Wang J, Zhang Y, et al. Berberine activates thermogenesis in white and brown adipose tissue. *Nat. Commun.* 5 (2014) 5493–5507.
- [30] Nishimura Y, Yoshinari T, Naruse K, Yamada T, Sumi K, Mitani H, et al. Active digestion of sperm mitochondrial DNA in single living sperm revealed by optical tweezers. *Proc. Natl. Acad. Sci. USA.* 103 (2016) 1382–1387.
- [31] Kilkeny C, Browne W, Cuthill IC, Emerson M, Altman DG. Animal research: reporting in vivo experiments: the ARRIVE guidelines. *Br. J. Pharmacol.* 160 (2010) 1577–1579.
- [32] McGrath JC, Lilley E. Implementing guidelines on reporting research using animals (ARRIVE etc.): new requirements for publication in BJP. *Br. J. Pharmacol.* 172 (2015) 3189–3193.
- [33] Pollard AE, Martins L, Muckett PJ, Khadayate S, Bornot A, Clausen M, et al. AMPK activation protects against diet induced obesity through Ucp1-independent thermogenesis in subcutaneous white adipose tissue. *Nat. Metab.* 1 (2019) 340–349.
- [34] Wang Z, Hu J, Yang X, Feng X, Li X, Huang L, et al. Design, synthesis, and evaluation of orally bioavailable quinoline-indole derivatives as innovative multitarget-directed ligands:

promotion of cell proliferation in the adult murine hippocampus for the treatment of alzheimer's disease. *J. Med. Chem.* 61 (2018)1871–1894.

Journal Pre-proof

Figure and Scheme Captions

Figure 1. Chemical structures of bouchardatine, **R17**, and 4 series of new β -indoloquinazoline analogues.

Figure 2. Evaluation of the lipid-lowering activity of β -indoloquinazoline analogues in 3T3-L1 adipocytes. After totally confluence, 3T3-L1 pre-adipocyte were exposed to differentiation cocktail I (a mixture of IBMX, dexamethasone, insulin) for 3 days, then switched to differentiation cocktail II (insulin) and incubated for another 3 days; compounds were diluted with the differentiation cocktail and added. At day 6, the TG level in the cells was determined by a TG assay or by staining with ORO working solution as described in Methods. **R17** and Metformin (1 mM) were viewed as the control compound. (A) Determination of the effects of derivatives on the TG level in 3T3-L1 adipocytes. The concentrations of derivatives were 1 and 5 μ M. (B) Representative microscopy images of the 3T3-L1 adipocytes were captured after compounds (1 μ M) were treated by ORO staining ($\times 200$). UND: undifferentiated group cells without the stimulation of an adipogenic cocktail. Ctrl (Control): differentiated group without treatment with the compounds. N = 4 independent experiments.

Figure 3. Inhibition of adipocyte differentiation and activation of AMPK by 4 potent compounds in 3T3-L1 adipocytes. (A) Confluent 3T3-L1 pre-adipocytes were treated with derivatives **11**, **20**, **21**, and **23** at 0, 0.01, 0.1, 0.3, 1, 3 and 10 μ M for 6 days during differentiation. On day 6, the intracellular TG content was determined *via* a TG assay and EC₅₀ values were calculated using

Origin 8 software (CA, USA). (B-F) Confluent pre-adipocytes were exposed to a differentiation cocktail for 24 h with or without the treatment of these potent derivatives (0, 0.01, 0.1 and 1 μM), cells were harvested and subjected to mRNA level of adipogenic markers and protein level of AMPK pathway by RT-qPCR and Western blot assay, respectively. (B-E) mRNA level of adipogenic markers C/EBP δ , C/EBP β , C/EBP α , and PPAR γ , the level of the gene of Ctrl group was viewed as 1. (F) AMPK activity determination. The expression levels of pAMPK α (Thr-172) were determined and quantified using Quantity One software. Protein levels were normalized to loading control Actin, the pAMPK α level of the Ctrl group was viewed as 1, compound treatment groups were calculated, and the high level of pAMPK α (Thr-172) indicates a higher activity of AMPK. N = 4 independent experiments.

Figure 4. Inhibition of adipocyte differentiation *via* AMPK pathway activation by **IQZ23**. (A) Confluent 3T3-L1 pre-adipocyte were exposed to an adipogenic cocktail in the presence or absence of **IQZ23** (1 μM) treatment during different periods of differentiation. At day 9, cells were collected for TG level determination. (B-C) Effects of **IQZ23** on the protein level of adipogenic factors and fatty acid synthesis related proteins in 3T3-L1 adipocytes. 3T3-L1 pre-adipocyte were exposed to the adipogenic cocktail in the presence of **R17** (1 μM) or **IQZ23** (0.3 and 1 μM) treatment. After treatment, cells were collected and expression levels of adipogenic factors (Day 1) and fatty acid synthesis related proteins (Day 6) were determined. (D-F) Effects of **IQZ23** on ATP synthase activity, ATP level and AMP-to-ATP ratio in 3T3-L1 adipocytes. 3T3-L1 pre-adipocyte were exposed to an adipogenic cocktail in the presence of **IQZ23** (0.3, 1 μM) treatment for 24 h, cells were collected and ATP synthase activity, ATP level, and AMP/ATP ratio were determined as described in Methods.

(G-H) AMPK knockdown abolishes the inhibition effect of **IQZ23** in 3T3-L1 adipocytes. After the cell density reached 80%, cells were transfected with 50 nM AMPK α siRNA for 24 h. After confluence, cells were exposed to adipogenic cocktail with or without **IQZ23** treatment for 1 day and 6 days, then cells were harvested and relevant parameters were determined. (G) Protein level of AMPK pathway and adipogenic factors after differentiation induction for 1 day. (H) TG level determination on Day 6. Values are expressed as the mean \pm SD. UND: undifferentiated group cells without the stimulation of an adipogenic cocktail. Control (Ctrl): differentiated group without treatment with the compounds. # $p < 0.05$, ## $p < 0.01$, ### $p < 0.001$, compared with UND group cell. * $p < 0.05$, ** $p < 0.01$, *** $p < 0.001$, compared with the control group. @ $p < 0.05$, @@ $p < 0.01$, compared with **IQZ23**-treated cells. N = 4 independent experiments.

Figure 5. Increase of insulin sensitivity in C2C12 myoblasts *via* AMPK pathway by **IQZ23**. (A-B) **IQZ23** increases glucose uptake distinguished from the insulin-signaling pathway. C2C12 myoblasts were treated with insulin (10 $\mu\text{g}/\text{mL}$), **IQZ23** (0.3, 1 μM), **R17** (1 μM), metformin (Met, 1 mM) alone or together for 6 h, then the culture medium was replaced with fresh medium containing 30 mM 2-NBDG and Hoechst 33342 (for nucleus, 1:1000) incubated at 37 $^{\circ}\text{C}$ for 30 min, the fluorescence intensity of 2-NBDG in cells was measured at the wavelength of Ex/Em of 465/540 nm, and representative images were captured using a Zeiss Microscopy System. Magnification, $\times 100$. The fluorescence in the control group was viewed as 1, and relative compound-treated group values were calculated. (C) Protein level of pAMPK α and AKT pathway in the cells treated with **R17** (1 μM), **IQZ23** (1 μM), insulin (10 $\mu\text{g}/\text{mL}$) or combination of each other, and quantification. (D-E) Effects of PI $_3$ K inhibitor LY-294002 (10 μM) on the glucose uptake and protein levels of PI $_3$ K/AKT

pathway in the presence of **IQZ23**. Cells were treated with **IQZ23** (1 μ M) or LY-294002 (10 μ M) alone or together for 6 h, and the glucose uptake was measured as described above and protein levels of pAMPK α and pAKT were determined and quantified. Values are expressed as the mean \pm SD. * p < 0.05, ** p < 0.01, *** p < 0.001, compared with the control group. [@] p < 0.05, compared with insulin-treated cells. N = 4 independent experiments.

Figure 6. Promotion of mitochondria biogenesis and oxidation capacity in 3T3-L1 adipocytes by **IQZ23**. (A-B) Effects of **R17** and **IQZ23** in mitochondrial contents in 3T3-L1 adipocytes. Cells were treated with AICAR (2 mM), **R17** (1 μ M), **IQZ23** (1 μ M) in the presence or absence of compound C (CC, 20 μ M) for 24 h, then cells were stained with hocheest 33342 (for nucleus, 1:1000) and mito-tracker (for mitochondria, 1:5000) at 37 $^{\circ}$ C for 30 min, the fluorescence intensity of Mito-tracker in cells was measured under the wavelength of Ex/Em of 579/599 nm and representative images were captured using a Zeiss Microscopy System. Magnification, \times 100. The fluorescence in the control group was viewed as 1, and relative compound-treated group values were calculated. (C) Effect of **R17** and **IQZ23** on the mRNA level of mitochondrial regulated genes. Cells were treated with **R17** (1 μ M) and **IQZ23** (0.3, 1 μ M) for 24 h, cells were collected and subjected to RNA extraction followed by RT-qPCR for the indicated genes assay. (D) Effect of **R17** (1 μ M) and **IQZ23** (1 μ M) on oxygen consumption in 3T3-L1 adipocytes as described in Method. * p < 0.05, ** p < 0.01, *** p < 0.001, compared with the control group. [#] p < 0.05, ^{##} p < 0.01, compared with AICAR, **R17** or **IQZ23** or treated cells. N = 4 independent experiments.

Figure 7. Amelioration of HFC diet feeding induced obesity and metabolic disorders by **IQZ23**.

Male C57BL/6J mice were fed with an HFC diet for 14 weeks, and **IQZ23** was administered in the last 6 weeks at a dose of 20 mg/kg every other day by *i.p.* injection; control group mice were injected with saline. GTT and ITT were determined at week 11 and week 13. After treatment, mice were anesthetized, plasma and tissues studied were isolated and weighted, and the chemicals in plasma were determined. (A) Appearance of mice. (B) Bodyweight. (C) Fat mass. (D) Total food intake during 6 weeks of treatment with **IQZ23**. (E) Acute effects of **IQZ23** on improved plasma glucose in mice. (F-G) GTT, ITT and the area under the curve (AUC). N = 15 mice in each group, values are expressed as the mean \pm SD. * p < 0.05, ** p < 0.01, *** p < 0.01, compared with CH group (fed with chow diet); # p < 0.05, ## p < 0.01, ### p < 0.01 compared with HFC group.

Figure 8. Inhibition of hepatic steatosis in HFC-mice by **IQZ23**. Male C57BL/6J mice were fed with an HFC diet for 14 weeks, and **IQZ23** was administered in the last 6 weeks at a dose of 20 mg/kg every other day by *i.p.* injection. After treatment, livers were isolated and weighed, and relative parameters were determined. (A) Liver weight. (B) Liver TG. (C) H&E and Oil red O staining in livers. N = 15 mice in each group, values are expressed as the mean \pm SD. * p < 0.05, ** p < 0.01, *** p < 0.01, compared with CH group; # p < 0.05, ## p < 0.01, ### p < 0.01 compared with HFC group.

Scheme 1. Synthesis of compounds **1-40**. Reagents and conditions: (i) K_2CO_3 , DMF, 160 °C, 2 h; (ii) 2 M NaOH, rt, 6 h; (iii) a: $SOCl_2$, 82 °C, 2 h; b: anthranilamide, Et_3N , 10 h, 0 °C; (iv) 2 M KOH, reflux, 8 h; (v) benzoperoxide, NBS, 90 °C, 24 h; (vi) DMSO, 100 °C, 2 h; (vii) $POCl_3$, 60 °C, 2 h; (viii) amines, Et_3N ; (ix) a: triethyl orthopropionate, 130 °C, 12 h; b: Br_2 , 60 °C, 4 h; c: phenyl

hydrazine, reflux, 10 h; d: PPA, 130 °C, 16 h; e: POCl₃, 100 °C, 4 h; (x) iodomethane/benzyl bromide, KOH; (xi) a: *N,N*-dimethylpropane-1,3-diamine, toluene, 80 °C; b: POCl₃, DMF, 1 h; (xii) a: (COCl)₂, rt, 1 h; b: anthranilamide, *t*-BuOK, 80-100°C; (xiii) POCl₃, DMF, 0°C→rt, 1 h; (xiv) thiol, K₂CO₃, 90 °C, 8 h; (xv) amines, K₂CO₃, (xvi) alcohols, NaH, rt, 1 h; (xvii) a: triethyl orthobutyrate, 130 °C, 12 h; b: Br₂, 60 °C, 4 h; c: phenylhydrazine, reflux, 10 h; d: PPA, 130 °C, 16 h. (xviii) POCl₃, DMF, 50-80 °C.

Table 1. Structures of the synthesized β -indoloquinazoline derivatives.

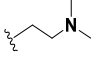
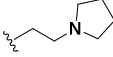
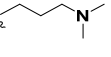
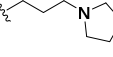
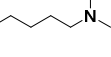
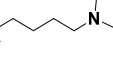
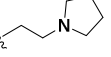
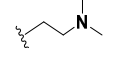
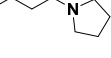
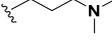
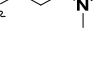
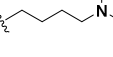
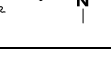
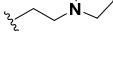
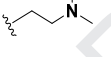
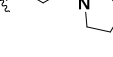
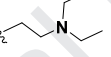
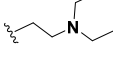
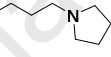
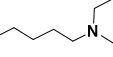
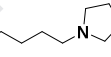
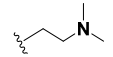
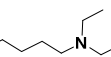
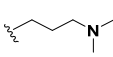
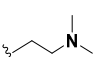
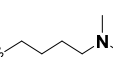
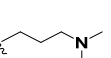
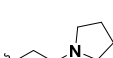
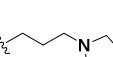
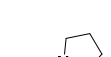
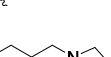
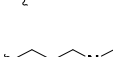
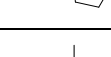
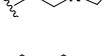
Series	compd.	X	Y	R	Series	compd.	X	Y	R
	1	O	NH			21	NH	NH	
	2	O	NH		□	22	NH	NH	
	3	O	NH			23	NH	NH	
□	4	O	NH			24	NH	NH	
	5	O	NH			25	NH	NH	
	6	NMe	NH			26	NH	NH	
	7	NBn	NH			27	NH	NH	
	8	NH	S			28	NH	NH	
	9	NH	S			29	NH	NH	
	10	NH	NH			30	NH	NH	
	11	NH	NH			31	O	O	
□	12	NH	NH		□	32	O	O	
	13	NH	O			33	O	O	
	14	NH	O			34	O	O	
	15	NH	O			35	O	O	
	16	NH	O			36	S	NH	
	17	NH	O			37	S	NH	
	18	NH	NH			38	S	NH	
□	19	NH	NH			39	S	NH	
	20	NH	NH			40	S	NH	

Table 2. Determination of aqueous solubility and rat liver microsomal stability of potent derivatives.

Compd.	Stability (%)	K (min ⁻¹)	<i>t</i> _{1/2} (min)	Cl _{int} ^a (μL/min/mg)	Aqueous solubility (μg/mL)
11	83.88	0.0028	247.6	2.8	15.1
20	84.02	0.0027	256.7	2.7	65.9
21	66.58	0.0066	105	6.6	56.4
23	80.69	0.0037	187.3	3.7	73.3
R17	71.05	0.0053	130.8	6.3	41.1
testosterone ^b			2.1		

^a Cl_{int}: intrinsic clearance.

^b The positive control testosterone exhibited metabolic stability that was consistent with the literature and internal validation data ³⁴.

Table 3. Pharmacokinetics assay of **23** and **R17** in SD rats^a

	23 (also named as IQZ23)		R17	
	<i>i.v.</i> (2 mg/kg)	<i>p.o.</i> (5 mg/kg)	<i>i.v.</i> (5 mg/kg)	<i>p.o.</i> (5 mg/kg)
$t_{1/2}$ (h)	4.4 ± 0.4	4.2 ± 0.3	3.14±0.5	5.1 ± 3.8
T_{max} (h)	NA	4.0 ± 0.38	NA	4.7 ± 1.2
C_{max} (ng/mL)	NA	37.1 ± 7.0	NA	23.75 ± 5.1
$AUC_{(0-t)}$ (h*ng/mL)	307.8 ± 17.0	374.1 ± 64.2	634.7 ± 19.7	246.9 ± 124.1
$AUC_{(0-\infty)}$ (h*ng/mL)	314.1 ± 18.2	383.6 ± 67.3	670.8 ± 9.3	293.9 ± 167.8
$MRT_{(0-\infty)}$ (h)	5.7 ± 0.3	7.5 ± 0.4	3.56 ± 0.3	9.62 ± 5.0
V_z (L/kg)	40.7 ± 3.1	NA	33.8 ± 5.7	NA
CL (L/h/kg)	6.4 ± 0.4	NA	7.5 ± 0.1	NA
F (%)		48.6 ± 8.3		43.8 ± 25.0

^a Pharmacokinetic parameters were calculated from plasma concentration–time data and are reported as Mean ± SD for n = 3.

Intravenous (*i.v.*) and oral (*p.o.*) pharmacokinetics were conducted in male SD rats. Solution formulation for *iv* and oral pharmacokinetics included 10% ethanol, 10% castor oil and 90% normal saline. NA = not applicable.

Table 4. Chronic effects of **IQZ23** on metabolic parameters in HFC mice ^a

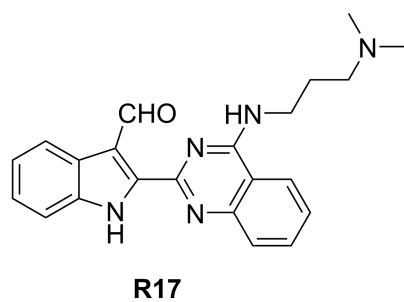
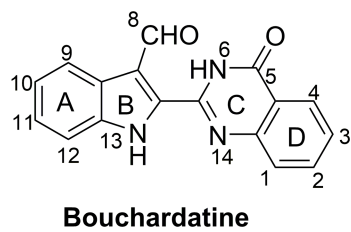
	CH-group	HFC-group	HFC- IQZ23 group
ALT (U/L)	49.6±1.5	231.9±18.5***	52±7.65 ^{###}
AST (U/L)	216.7±9.7	341.6±23.8***	163.7±17.27 ^{###}
ALB (mM)	35.9±1.1	38.7±1.8	30.4±4.4 [#]
TBIL (mM)	1.1±0.07	1.3±0.12	0.9±0.2 [#]
BUN (mM)	11.6±1.5	14.6±1.4**	11.5±1.0 ^{##}
CRE (μM)	16.3±0.5	14.9±2.8	14.5±2.0
Glucose (mM)	9.7±0.29	11.8±1.3**	9.3±1.1 ^{##}
FFA (μM)	452.1±23.6	1668.5±144.6***	694.4±69.0 ^{###}
TG (mM)	0.9±0.06	1.2±0.02**	0.92±0.2 [#]
CHO (mM)	3.4±0.2	6.2±0.3**	4.7±0.6 [#]
Insulin (ng/mL)	1.96±0.2	3.5±0.6**	2.2±0.5 ^{##}
LDL-c (mM)	0.4±0.03	0.9±0.4**	0.81±0.15
LDL-c/HDL-c	0.2±0.02	0.4±0.13**	0.25±0.05 ^{##}

^a HFC mice were treated with **IQZ23** by *i.p.* at the dosage of 20 mg kg⁻¹ each other day for 6 weeks, the

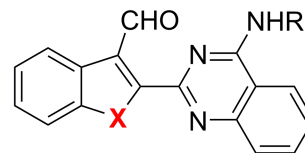
HFC-control mice were administrated with the saline. The results were expressed as the mean ± S.D. N = 15 mice

each group. ^b Fasting blood glucose. **p* < 0.05; ***p* < 0.01; ****p* < 0.001 vs CH group mice; #*p* < 0.05; ##*p* < 0.01;

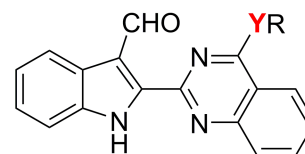
###*p* < 0.001 vs HFC group mice.



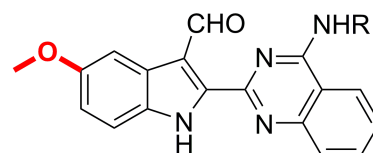
checking the importance
of NH in indole ring



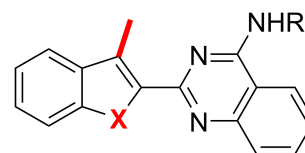
expanding the types of
side chain at 5-position



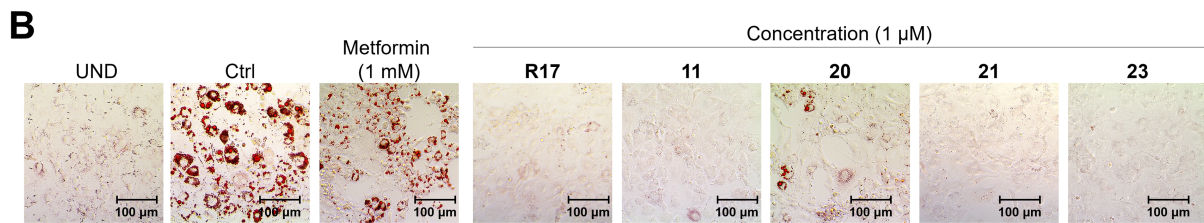
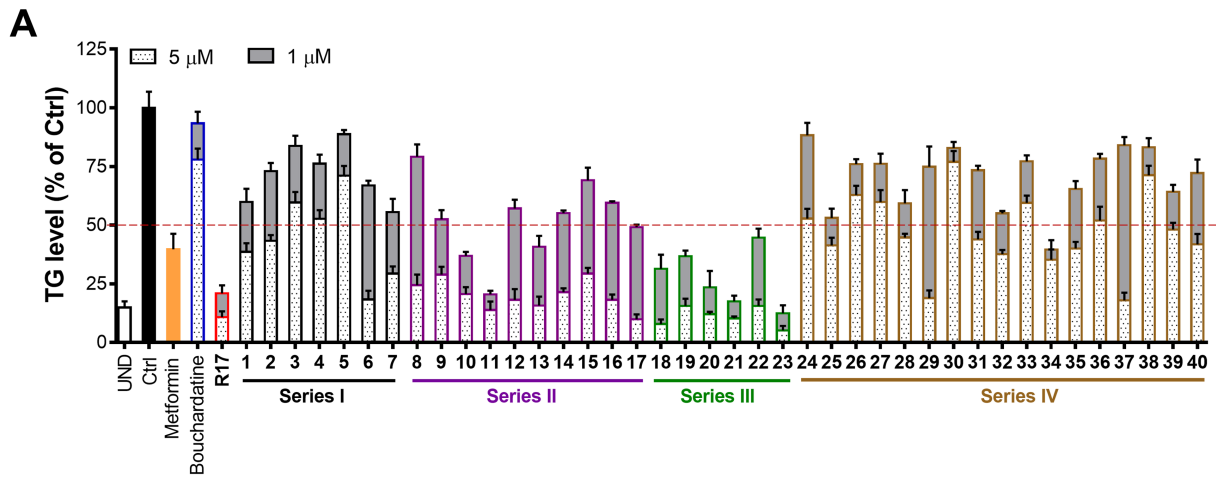
introducing meoxyl group
at 10-position

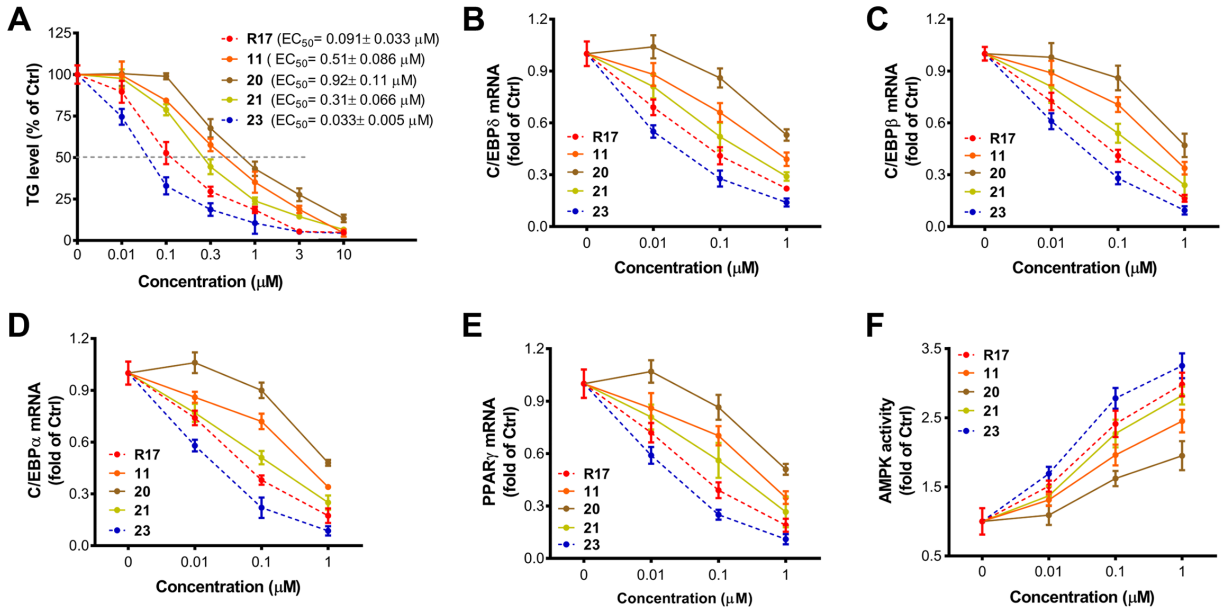


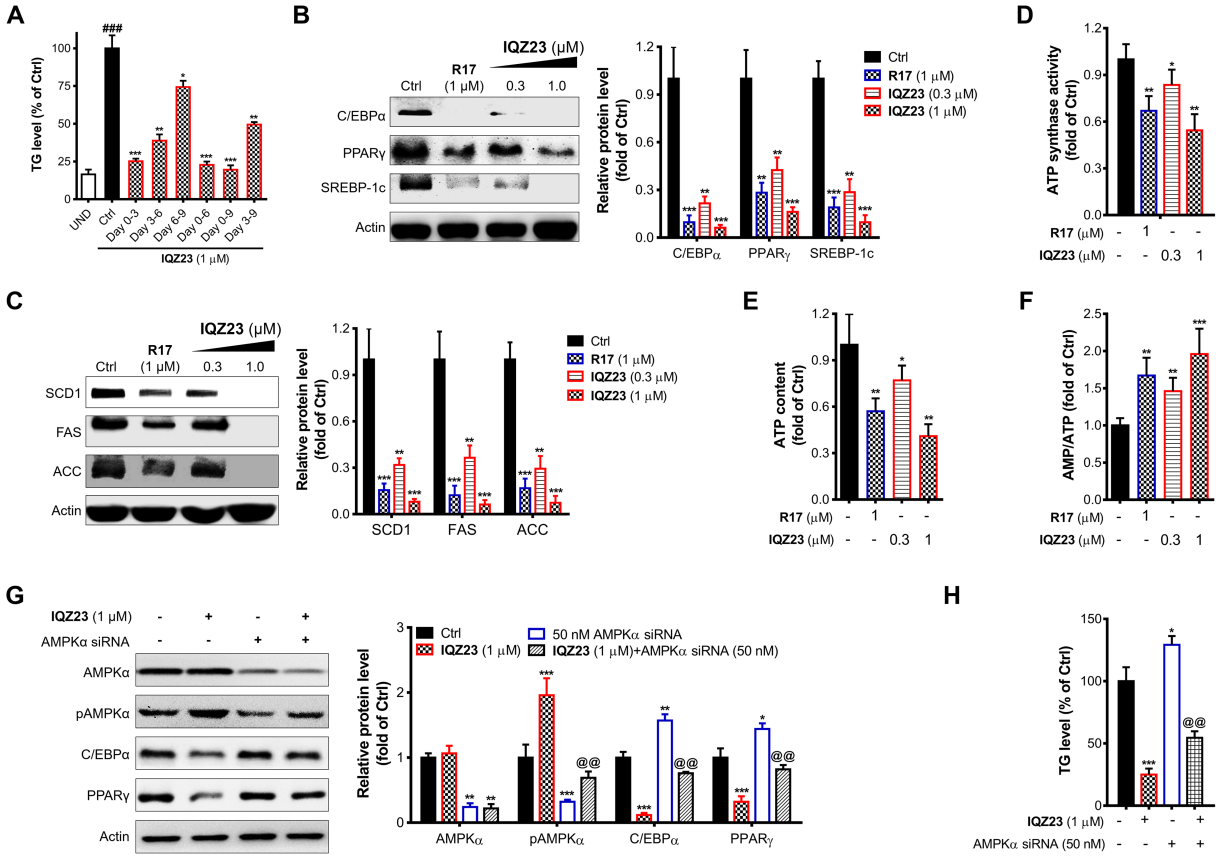
changing CHO into CH₃
and NH into O or S

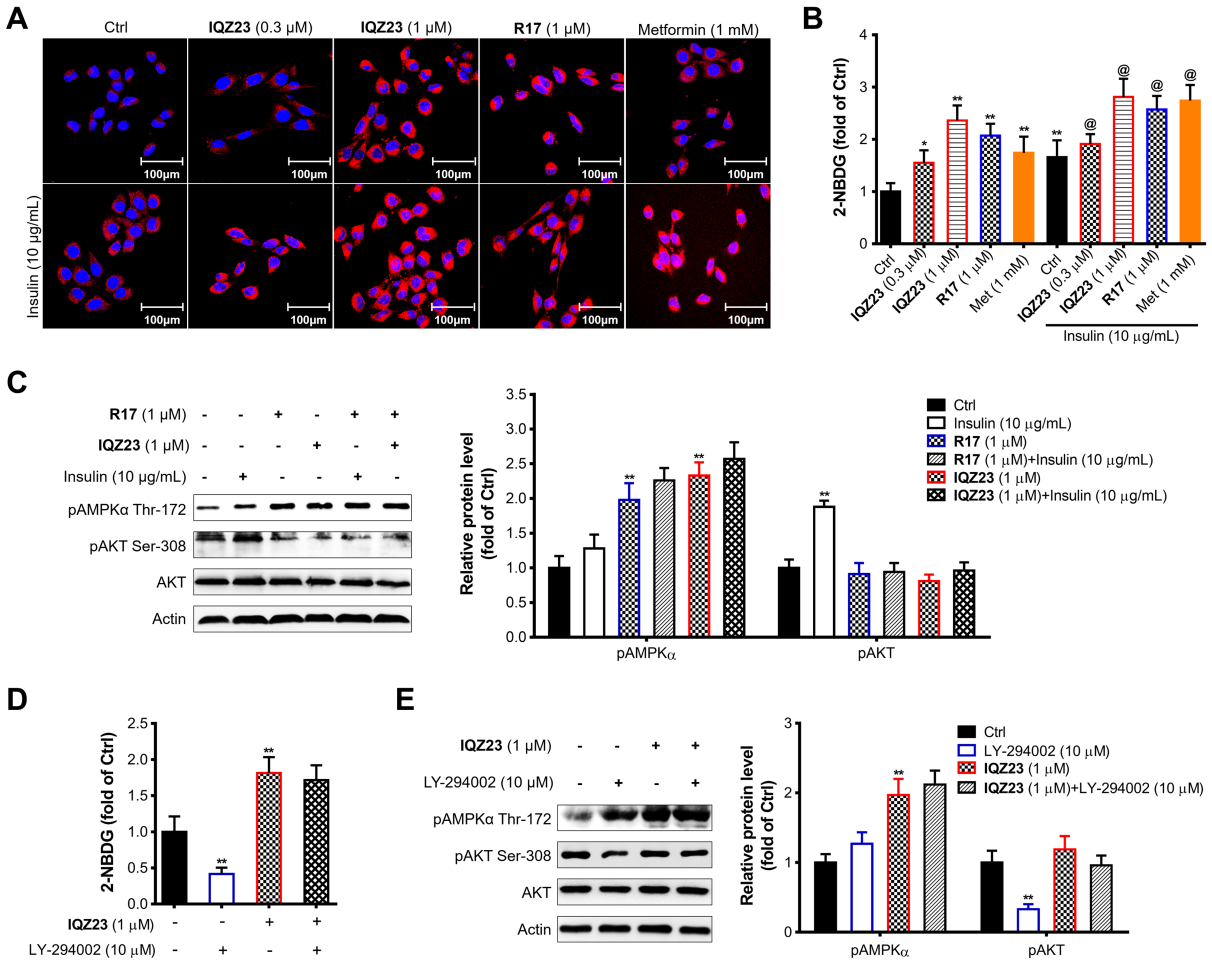


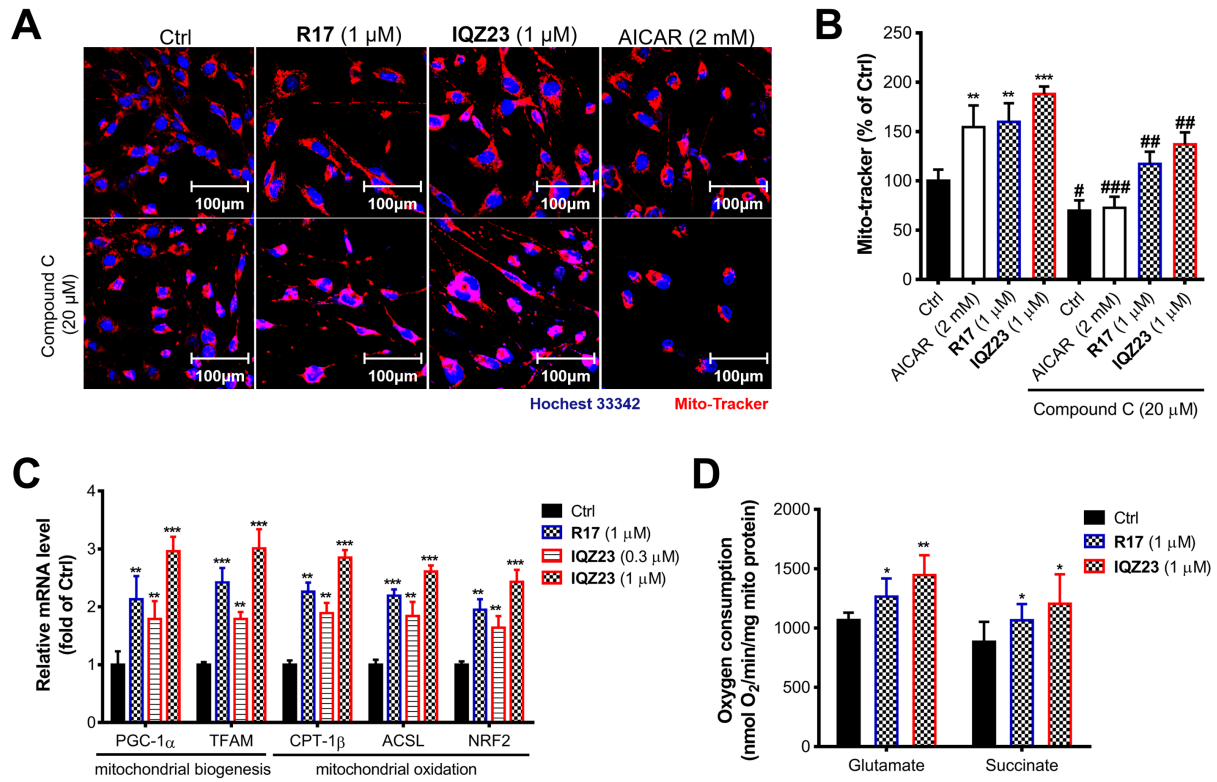
Journal

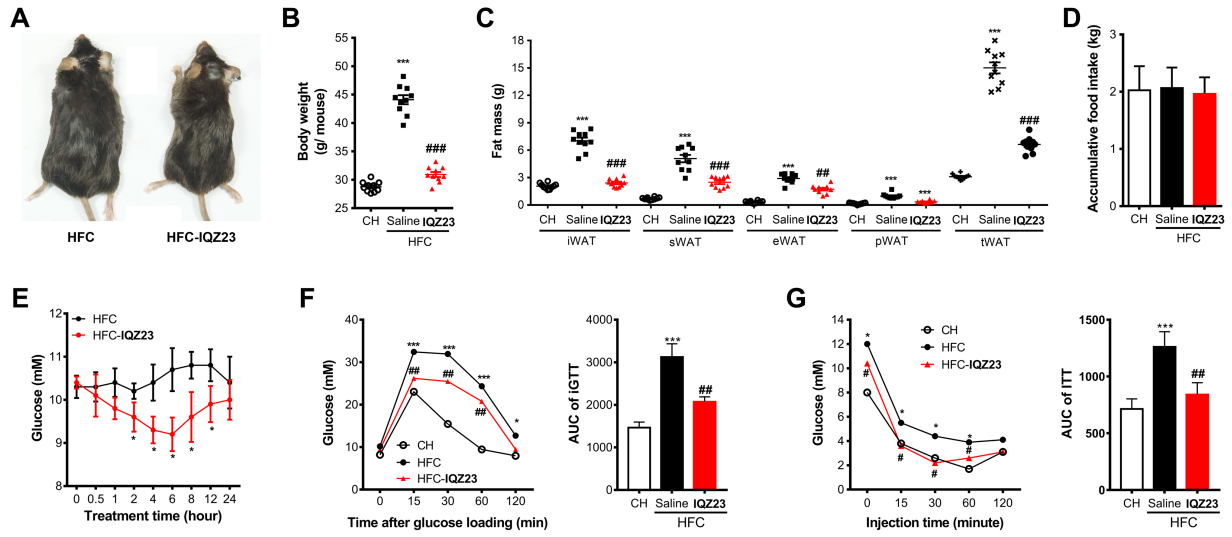


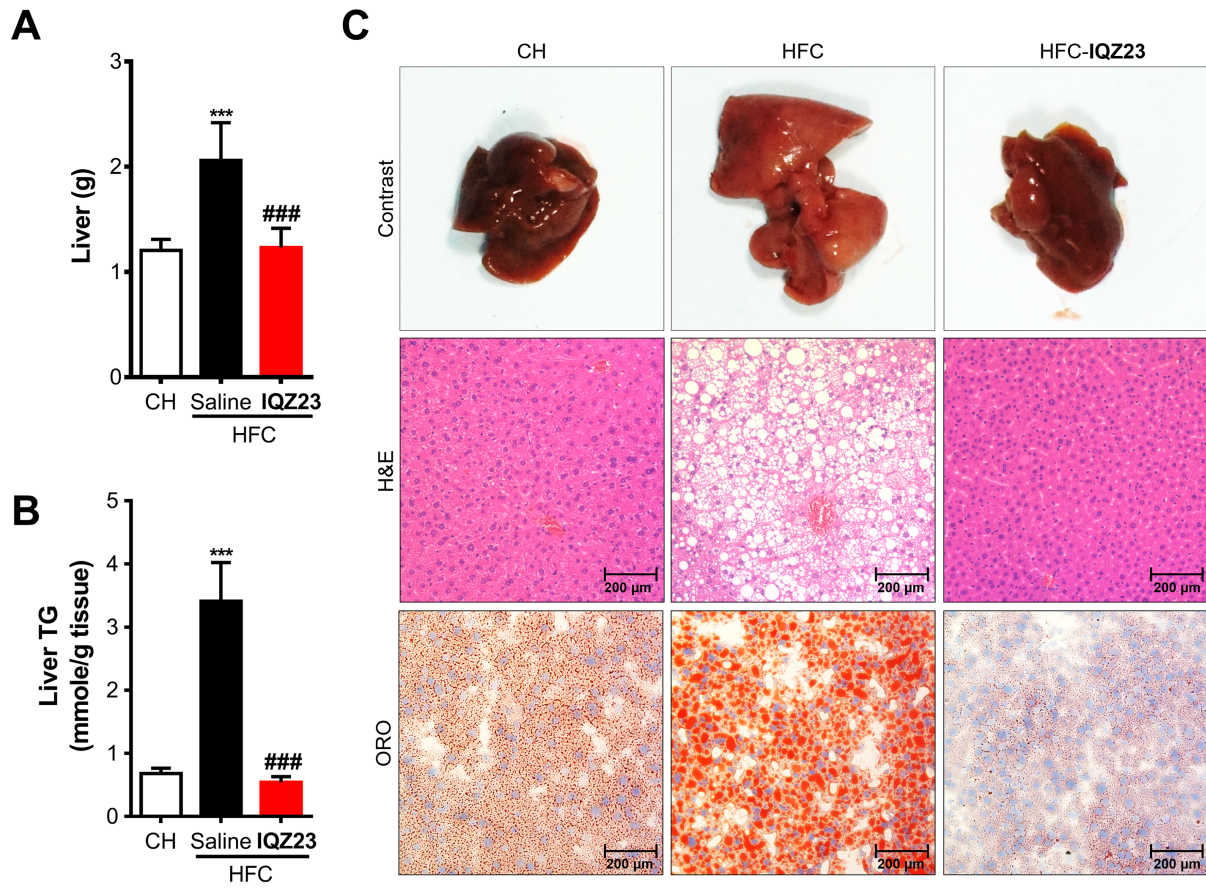


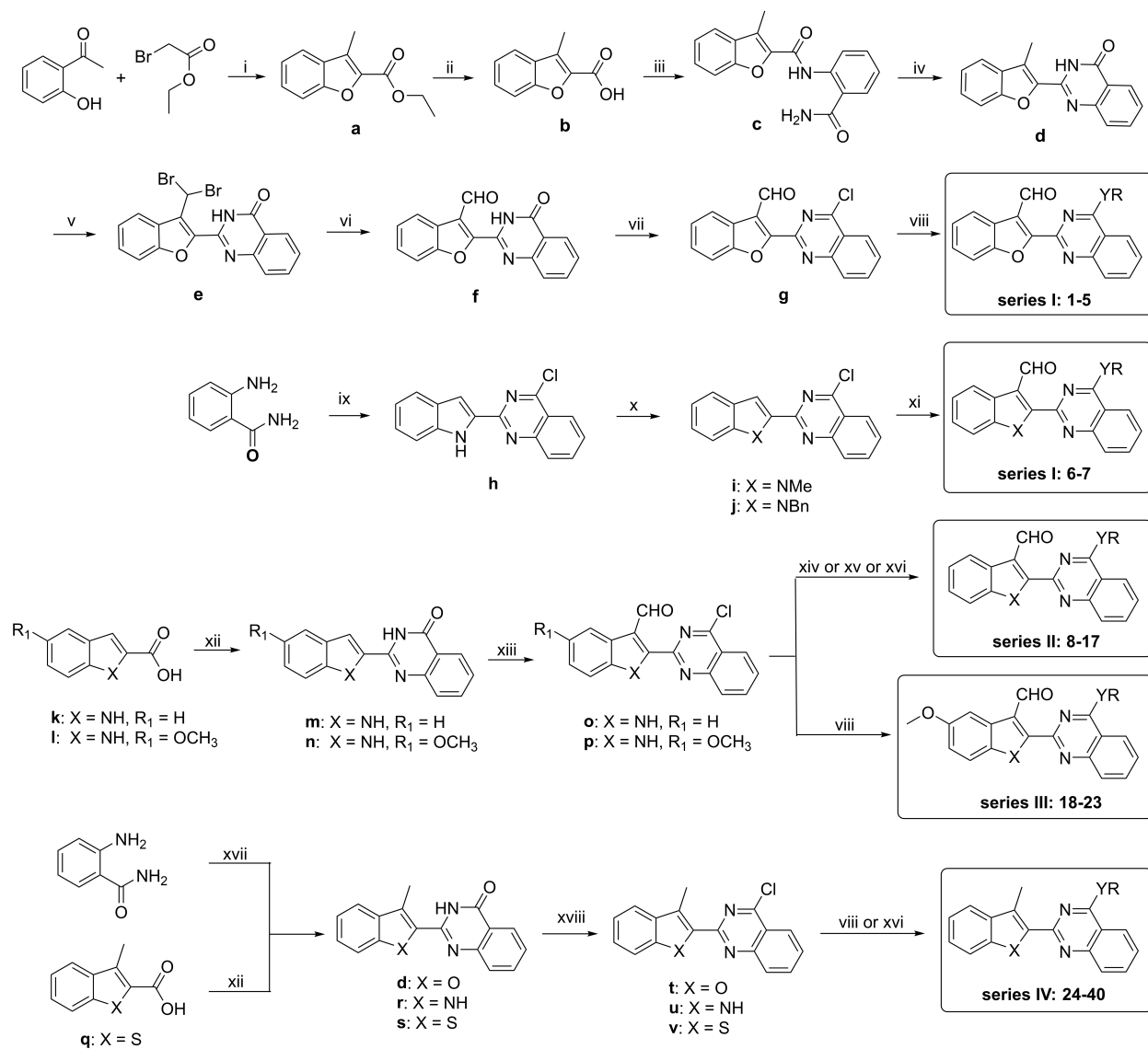












Highlights

- ✧ 40 novel novel β -indoloquinazoline analogs were designed and synthesized.
- ✧ The lipid-lowering activity was evaluated based on 3T3-L1 adipocyte model.
- ✧ Compound **IQZ23** shows a good drug-like properties and effectiveness on obesity mice.
- ✧ Compound **IQZ23** activates AMPK pathway by modulating ATP synthase activity.

Journal Pre-proof

Declaration of interests

The authors declare that they have no known competing financial interests or personal relationships that could have appeared to influence the work reported in this paper.

The authors declare the following financial interests/personal relationships which may be considered as potential competing interests:

Journal Pre-proof